The Collection of Ice in Jet A-1 Fuel Pipes

by

Thomas C. Maloney

A thesis submitted to the

Graduate School-New Brunswick

Rutgers, The State University of New Jersey

in partial fulfillment of the requirements

for the degree of

Master of Science

Graduate Program in Mechanical and Aerospace Engineering

written under the direction of

Dr. Tobias Rossmann

Dr. Fransisco J. Diez

and approved by

_____

_____

_____

_____

New Brunswick, New Jersey

October, 2012

Abstract of the Thesis

The Collection of Ice in Jet A-1 Fuel Pipes

by Thomas C. Maloney

Thesis Directors:
Dr. Tobias Rossmann
Dr. Fransisco J. Diez

Ice collection and blockages in fuel systems have been of interest to the aerospace community since their discovery in the late 1950's when a B-52 crashed. A recent growth of interest was provoked by several incidents that occurred within the last few years. This study seeks to understand the underlying principles of ice growth in fuel flow systems.

Tests were performed in a recirculated fuel system with a fuel tank that held approximately 115 gallons of Jet A-1 fuel and ice accumulation was observed in two removable test pipes. The setup was in an altitude chamber capable of -60 °F and the experiments involved full scale flow components.

Initially, tests were done to better understand the system and variables that effected accumulation. First, initial conditions within the test pipes were varied. Next, pipe geometry, pipe surface properties, initial water content of the fuel and heat transfer from the fuel pipe were varied. As a result of the tests, observations were made about other effects involved in the study. The effects include: the result of sequentially run tests, the effect of the fuel on the freezing temperature of the entrained water, the effect of ice accumulation on pipe welds, and the effect of the test pipe entrance and exit flow conditions on ice accumulation. The results of initial tests were qualitative.

Later quantitative tests were done to demonstrate the dependence of temperature, Reynolds number, and heat transfer on ice accumulation. Tests were quantified with a pressure increase across the pipe sections that was normalized by the expected

theoretical initial pressure. As a result of these tests the effect of contamination in the fuel was revealed.

For ease of reference, the initial tests were called "stage I" and the later tests were called "stage II".

The results of stage I showed that accumulation of soft ice was greatest when a layer of hard ice had initially formed on the pipe surface. Stainless steel collected more ice than Teflon® and there was a lack of a preferential accumulation region downstream of a pipe bend. A greater heat transfer from the pipe increased ice accumulation for aluminum that was made rough with 80 grit sand paper, and for Teflon®. Water was shown to collect in the pipe system as the number of tests increased and the freeze temperature of either the hard or soft ice was about 0 °C. Finally, results of "stage I" tests showed that stainless steel pipe welds were a preferred sight for ice to accumulate.

Repeatability was done first in stage II and the normalized pressure increase for two 3/4″ un-insulated pipe tests were within 7%. Normalized pressure increase across a pipe was shown to increase as Reynolds number decreased. A 50% increase in Reynolds number led to a 40% decrease in characteristic normalized pressure increase (CNPI). Tests were done at three temperatures and ice accumulated the most at -11 °C. The CNPI at -11 °C was about three times greater than the CNPI at -7.4 °C and about sixty times greater than the CNPI at -19.4 °C.

A greater heat transfer from the fuel pipe increased ice accumulation. For the amount of time that the tests ran, the total normalized pressure increase was about .9 greater for an un-insulated pipe than for an insulated pipe.

Contamination in the fuel increased the amount of soft ice that collected in the system. The CNPI for the more contaminated fuel was more than double the case with less contaminated fuel.

Possible solutions for the prevention or decrease of ice accumulation in aircraft

fuel systems based on the results of this study are insulated pipes, a change in the type of pipe material, a higher fuel flow rate and cleaner fuel. The fuel temperature could also be altered to avoid temperatures where the most ice accumulates.

Acknowledgments

I would like to thank both of my professors, Dr. Rossmann and Dr. Diez for their guidance and advice in this project. The project may have taken substantially longer if it were not for the push that I was given early in the project. Thank you for the weekly meetings where I could learn from two people who had done this before and who were easily able to incorporate textbook knowledge into application.

I would also like to thank Dr. Yogesh Jaluria for taking the time to be a committee member for my public examination.

I thank Bill Cavage for construction of much of the experimental setup. His design was the basic structure that the final experimental setup evolved from.

Thanks to my family for their support throughout this project. Especially my grandfather and mom who let me stay with them for a little while.

I thank Dave Mills for assistance with the set up of the experiment and advice for how things could be better. I thank Rob Ochs and Dick Hill for advice about presentations and the semantics of how the FAA and the Rutgers grad assistantship work. I also thank them for their will to help whenever I had a question. I thank Joey DeFalco for use of his tools and for the introduction that he gave me the first month that I was at the FAA. Thanks to Tom and Wayne at the machine shop for the parts that they made and lessons about equipment.

I thank everyone else in fire safety that I may have asked a question to or may have helped in the project (Steve, Eddie, Pat). I thank the FAA for use of their

facilities.

Contents

List of Tables

List of Figures

1. Introduction

This chapter provides background for this study and scientific information useful to understand ice accumulation. Later in this chapter the objectives are introduced.

1.1 Background and Motivation

The accumulation of ice in fuel lines has had ongoing interest within the aerospace industry throughout the world. Accumulation occurs when water within jet fuel collects on the inside surface of fuel pipes in the form of ice. Many studies have been carried out in an attempt to understand this phenomenon. The accumulation can be hazardous if the ice separates from the pipe and clogs downstream fuel components. For this study, the accumulation rather than the detachment of ice is the main focus.

The problem was first discovered by the Air Force in 1958 when a B-52 crashed on a day that the air temperature was below zero Celsius in South Dakota (figure 1.1). This resulted in a few deaths. Once the problem was discovered, over 200 previous aircraft accidents were attributed to the accumulation of ice in fuel systems [23]. Since then, various fuel system modifications have been implemented which include fuel heaters and anti-icing additives.

A more recent plane crash attributed to fuel pipe icing was a Boeing 777, with registration G-YMMM, in its descent into Heathrow International Airport in London. The accident investigation concluded that before the crash, ice had collected on the inside of the fuel system. When the plane was on final approach the ice released and

Figure 1.1: B-52 crash caused by ice in the fuel [23]

blocked the FOHE (Fuel Oil Heat Exchanger). This blockage caused the plane to experience an "uncommanded" decrease in thrust and crash one thousand feet short of the runway. No lives were lost in this accident [3].

Figure 1.2: Boeing 777 crash caused by ice in the fuel [26]

The amount of water that was determined to be in the fuel prior to the crash was seventy parts per million plus some that may have entered through vents during flight [3]. The temperature during the flight was below average but it was not the coldest that this plane had encountered. The fuel temperature for this flight reached

a minimum of -32 °C and had an initial temperature of -2 °C [3].

Prior to the uncommanded decrease in thrust of the first engine, the fuel flow experienced a local maximum. This peak may have contributed to the release of ice. Seven seconds later the second engine experienced rollback (a decrease in thrust) [3].

Another Boeing 777 experienced an ice induced decrease in thrust on the 26th of November 2008 while in flight but was able to recover and prevent a crash. It has been concluded that this Boeing 777 also had the ice blockage occur on the FOHE [3].

More recently, on the 19th of May 2009, an A330 experienced a decrease in thrust on its #1 engine. It was again concluded that the rollback was caused by ice that had clogged a component in the fuel system [8].

In response to these occurrences the U.S. Air Force, Boeing, Thornton Research Center, CRC, the Navy, Cranfield University in collaboration with EADS Innovation Works and Airbus, the FAA and others have contributed to research and understand ice accumulation in fuel.

The Air Force determined that the type of ice is dependent on the rate of cooling, water droplet size of entrained water and agitation. They also observed that some water droplets in fuel become supercooled [3]. A method that they found effective to clear a fuel system was to inject AN-A-18 alcohol [14]. They provided the SAE with information to develop guidelines for running tests. The information was provided in two documents, *Aerospace Information Report (AIR) 790* and *Aerospace Recommended Practice (ARP) 1401* [3].

AIR 790 states that experimental setups should have configurations and conditions that represent the actual situation experienced by and aircraft. This document also gives recommendations for the introduction and circulation of water in the fuel system. It suggests that the fuel be conditioned by water injection and states that single pass systems without recirculation of fuel are preferred. The second document (ARP

1401) gives further recommendations for specific procedures for tests and provides more information about water injection into the fuel system [3].

A test with Boeing 777 fuel pipes was conducted by Boeing. Conclusions from their experiments attribute ice accumulation to occur when the ice in the fuel has a sticky consistency between -5° and -20° Celsius [3].

Tests done at the Thornton Research Center of the Shell Aeronautical Laboratory in England found that addition of isopropyl alcohol at concentrations of .5% to 1% was effective as an antifreeze [14].

Tests done for the Coordinating Research Council showed a correlation between the cloud point of the fuel and the temperature that the fuel filter became clogged. They also found that fuels with suspended water will cause a filter to clog slightly below 0 °C [14].

Tests done at Lockheed showed that ice in fuel clogged a micronic filter at about -9.4 °C.

The Navy showed the effect of various fuel additives for prevention of ice blockage of a filter. They also characterized the water retention of various characteristic fuel hydrocarbons. They provided time scales for the uptake of dissolved water into fuel and withdrawal of water from supersaturated fuel [14].

More recent tests were quiescent ice accumulation tests and fuel tests performed at Cranfield University. They showed that water in fuel accretes directly from the dissolved phase onto a sub-cooled surface [16].

Murray, Broadley, and Morris showed that micron sized water droplets in quiescent Jet A-1 fuel would supercool and freeze at temperatures around -36 °C [19].

The work done previously by the FAA showed that ice would not accumulate on the inside of an aluminum pipe when fuel system icing inhibitor (ethylene glycol monomethyl ether) was in the fuel. They also showed that ice would not accumulate when fuel was introduced at a temperature below 0 °C, into a pipe system. The tests

of this paper are a continuation of previous FAA tests.

There have been tests performed related to ice nucleation that were not specifically for the accumulation of ice in jet fuel pipes that may be applied to this research. This work includes textbook information about ice nucleation and growth and studies performed to determine adhesion forces of ice to materials. Laforte and Beisswenger [15] determined the adhesion force of ice to an assortment of materials and Jellinek [12] determined the adhesion force of ice to stainless steel. Another topic that may provide information relevant to ice accumulation in fuel pipes is atmospheric physics, such as cloud formation and growth of ice particles in the atmosphere.

1.2 Review of Relevant Concepts

This section describes scientific information relevant to ice accumulation in jet fuel pipes. It explores information about the fuel, ice, temperature, water, pipe materials, thermodynamics and fluid dynamics relevant to this phenomenon.

1.2.1 Variation of Temperature with Altitude

For ice to form, temperature has to be cold enough. As altitude above sea level increases, the ambient temperature tends to decrease. A typical commercial aircraft may climb to thirty five thousand feet. At this altitude, the plane is near the top or possibly outside of the troposphere. At the top of the troposphere is an altitude called the tropopause. This begins a region that has a constant temperature of approximately -56.5 °C [29].

Two important parameters that affect the resultant surface temperature of the aircraft are the adiabatic wall temperature and the stagnation temperature. Although ambient conditions outside the aircraft may be -56.5 °C, this would not be the surface temperature of the aircraft body. As the aircraft is moving at a sufficient velocity,

the approximate temperature of the plane outside surface is the adiabatic wall temperature. At the stagnation point, or front of the wing, the temperature would be the stagnation temperature. These two quantities are approximately equal. For an aircraft with an ambient static air temperature of -56.5 °C and Mach number of .8, the stagnation temperature is about -49.57 °C. The ambient temperature may be 70 °C different than the fuel temperature so there is potential to have a high heat transfer rate from the fuel and easily reach temperatures required for ice formation and growth.

1.2.2 Ice

Ice may exist in sixteen different crystalline forms and three non-crystalline forms [5]. The crystalline forms are numbered I-XV and the 16th form exists because number I may be hexagonal or cubic. A diagram with some of the forms is shown in figure 1.3 In general the type of ice that one would encounter is a function of temperature and pressure. The most common type of ice that is found at atmospheric conditions is hexagonal, often written as I_h. Although rare, another type of ice that has been found to exist in typical flight conditions is cubic ice. It is however expected that any cubic ice that forms will convert to hexagonal ice because of the temperature-pressure dependence of cubic ice [10]. It is possible that the presence of fuel may shift the freezing temperature of ice slightly but from tests performed by Cranfield University, Boeing, Airbus etc. the temperature change is less than 5 °C.

1.2.3 Jet Fuel and Constituents

Jet A-1 is the fuel that is used in this study. It is processed in accordance with Defence Standard 91-91. The standard limits some of the fuels components and properties. Table 1.1 shows some selected specifications.

There are infinite variations of what may actually exist in a given sample of Jet

A-1. The fuel is required to meet certain thermodynamic specifications and can therefore have infinite variations of the four main hydrocarbons.

The four main hydrocarbons and a composition at which they may typically exist are as follows: n-paraffins: 19%, i-paraffins: 31%, cycloparaffins: 31%, aromatics: 19% [7]. There is however a restriction for the composition of aromatics. Aromatics are allowed to exist in jet fuel at a maximum of 25% [11].

Jet fuel can exist in a synthetic or semi-synthetic form which may further alter the water retention and ice handling properties of the fuel [24]. Not much is known about ice accumulation in synthetic or semi-synthetic jet fuel pipes.

Additives, such as static dissipater additive, antioxidant, metal deactivator, lubricity additive, fuel system icing inhibitor and +100 additive may also be present in jet fuel [2]. This thesis does not indicate how these additives contribute to water retention or ice formation aside from what was previously done by the FAA with fuel system icing inhibitor.

Organic compounds containing sulfur, nitrogen, or oxygen, trace amounts of metals, sediment and microbial growth may also be found in jet fuel [22]. The maximum amount of sulfur that is allowed to exist in Jet A-1 is .3% by mass. The maximum amount of "particulate contamination at the point of manufacture" is 1 mg/Liter [24].

Surfactants may be present naturally in fuel or as a consequence of contamination. Surfactants reduce entrained water droplet size and therefore decrease the velocity that a droplet will settle. Surfactants may cause water separation coalescers to be ineffective because the smaller droplets may more easily pass through pathways in the coalescing media; the water droplet size may become too small for the specification of the filter element [31].

Table 1.1: Selected Specifications for Jet A-1 [24]

Visual Appearance	Clear, bright and visually free from solid matter and undissolved water at ambient fuel temperature
Particulate Contamination, at point of manufacture	Max 1.0 mg/l
Total Acidity	Max 0.015 mg KOH/g
Aromatics	Max 25.0% v/v
Sulfur, Total	Max 0.30% m/m
Sulfur, Mercaptan	Max 0.0030% m/m
Density at 15 °C	Min 775.0 kg/m3; Max 840.0 kg/m3
Freezing Point	Max minus 47.0 °C
Viscosity at minus 20 °C	Max 8.000 mm2/s (cSt)

1.2.4 Water Solubility of Jet Fuel

In a test performed by Krynitsky et al. [14] at 60 °F, Toluene (an aromatic) held 407 ppm water and n-octane (a paraffin) held 46 ppm water. The combination of hydrocarbons mentioned in 1.2.3 lead to a typical water concentration that Jet A-1 may contain of 100 ppm [31].

The amount of water that will dissolve in jet fuel varies with temperature. Jet fuel at a higher temperature has the potential to hold more dissolved water than jet fuel at a lower temperature. Figure 1.4 shows how the water saturation level in aromatics (toluene and xylene) and paraffins (kerosene) vary with temperature [13]. When a saturated fuel is cooled, dissolved water forms small droplets that suspend themselves in the fuel. Water in this form is commonly called entrained water. The approximate diameter of the entrained water droplets is ten microns for AN-F-58 fuel [14]. Over time these droplets settle to the bottom of the fuel tank and collect. Krynitsky et al. [14] showed that when AN-F-58 fuel is cooled, 50% of the resultant entrained water settles in the first day and after 6 days 4% still remains. The collection or puddle of water is commonly called free water.

1.2.5 Ice Accumulation Overview

The process of ice collection on the inside of the fuel pipes may be described in steps. After water enters the fuel, the temperature of the fuel/water mixture is lowered. While the fuel/water mixture is above the freezing temperature of the water, entrained or free water may accumulate on the inside of fuel pipes. When the mixture temperature decreases below the freezing temperature of the water, the water begins to freeze. As fuel continually flows through the pipe, ice continues to accumulate.

Water Accumulation in Fuel

Some water is present in the fuel prior to delivery to the plane, though tests are set up to limit how much may be in the fuel upon delivery [3]. When the fuel mixture is loaded onto the plane it exchanges moisture with the atmosphere through vents. At this time the fuel has the potential to come into equilibrium with ambient humid air.

The amount of water in the fuel can be further increased as flights increase. When the fuel drops in temperature, entrained water may settle to the bottom of the tank. When the plane arrives at its destination it refuels and the cycle repeats itself. This may explain the free water that was found in the bottom of the G-YMMM fuel tank [3].

Tests done by [14] showed that a static sample of fuel with water at the bottom would grow from 57% saturation to 99% saturation in six hours. They also showed that a fuel sample could be shaken for one minute and then allowed to rest for fifteen minutes and have the water saturation level grow from less than 57% to near saturation. These results, when compared with the time required for water to settle as mentioned previously, indicate that free water may enter fuel faster than entrained water leaves it.

Water Accumulation on the Inside of Fuel Pipes

While jet fuel cools, entrained water and free water stick to the inside of fuel pipes because of adhesion forces. When the temperature of the super-saturated fuel drops below the freeze temperature of the water, the ice may accumulate in two ways: supercooled water may use the pipe material as a nucleation site and/or ice particles may stick to the pipe surface or ice surface. Ice accumulation begins with ice or supercooled water collection on the pipe material and evolves into ice or water collection onto a layer of ice.

Quantification of Ice Accumulation

Fuel flow restriction increases with ice accumulation. The amount of ice can be quantified with differential pressure measurements.

There are several parameters that contribute to pressure drop across a pipe section. These parameters are gravity, density, friction factor, length, and diameter. The relation is solved by integration of the viscous head equation with some simplifying assumptions. The result for the pressure drop between two points in a pipe is given by equation 1.1. This equation assumes constant pipe diameter and therefore constant velocity.

$$P_b - P_a = -\rho g \left(\Delta z + f \frac{L}{D} \frac{V^2}{2g} \right) \tag{1.1}$$

The friction factor f, for turbulent flow, is a function of Reynolds number: Re, roughness height: e, and diameter: D and is given by the Colebrook equation: equation 1.2.

$$\frac{1}{\sqrt{f}} = -2log \left(\frac{e}{3.7D} + \frac{2.51}{Re\sqrt{f}} \right) \tag{1.2}$$

As ice accumulates on the inside surface of a pipe, there are two major influences

that effect pressure drop. A growth of non-uniform ice specks on the wall would increase the roughness height of the pipe and a uniform distribution of ice on the inside wall would decrease the pipe diameter.

1.2.6 Nucleation

Nucleation occurs in homogeneous and heterogeneous forms. Because water needs to reach temperatures of about -40 °C to nucleate homogeneously the problem of ice collection on the inside of fuel pipes is almost entirely heterogeneous nucleation dependent. The fuel may reach homogeneous nucleation temperatures in rare extreme cases [19]. In these cases however, a greater concern is of the fuel itself beginning to wax.

Prior to ice nucleation, supercooled water exists in the form of ice germs. These are small clusters of H_2O similar to ice. Depending on the level of fuel saturation, the germs can grow and decay in size until they reach a critical size which allows them to nucleate with a heterogeneous particle or material [25]. Once the initial ice freezes, it can grow larger through the process of deposition. With deposition, dissolved water from the fuel contributes to the ice growth.

1.2.7 Contributors to Ice Accumulation Rate

There are additional factors that contribute to fuel pipe icing. The rate at which *ice and water* accumulate on the inside of a fuel pipe is dependent on pipe material, pipe surface properties, temperature, fuel flow turbulence, agitation and the fuel/water mixture Reynolds number. The rate at which *ice* accumulates is also dependant on the rate of cooling of the fuel/water mixture and electric fields.

Dependence of Ice and Water Accumulation on Pipe Material

An important parameter that governs ice nucleation is contact angle. The contact angle is generally described as the angle a water droplet makes with a surface (illustrated in figure 1.5 by θ_c). It exists due to the balance of cohesion forces within the liquid and the adhesion force between the liquid and solid.

The rate of ice and water accumulation depends on pipe material. The temperature of heterogeneous nucleation for supercooled water with a pipe material is dependent on the contact angle of the water droplet. The heterogeneous nucleation temperature for supercooled water with a material increases as contact angle decreases.

The adhesion force of water to a pipe material, commonly called hydrophobicity, is also related to contact angle. A material will accumulate less water if it is more hydrophobic because of a smaller adhesion force between the material and water. Hydrophobicity increases with contact angle. An approximation for the contact angle of water with stainless steel is 72° [1].

Upon contact with the dissimilar pipe material, suitable conditions can cause heterogeneous nucleation to occur. This happens because the pipe acts as part of the H_2O radius and increases the germs effective size. Different materials have varying contact angles with the water droplets and therefore affect the size and amount of energy required for nucleation. According to this simplified model, if the pipe material was very hydrophobic and therefore had a very large contact angle, water would be much less likely to accumulate on the pipe walls.

Ice that has formed on a relatively hydrophobic material could have lower bond strength with the pipe and therefore be less likely to significantly accumulate. Laforte and Beisswenger [15] showed that the application of various material coatings to a beam changed the force at which ice would stick to it.

The similarity of the crystal structure of ice and the structure of a pipe material

may also contribute to ice accumulation in fuel pipes [25].

Dependence of Ice Accumulation on Pipe Surface Properties

The surface properties of a pipe material affect the rate of ice accumulation. A pipe with a rough surface (greater than microscale roughness) may have less contact with an ice particle than a pipe with a smooth surface. Rough pipes may therefore have less contact force with ice particles and therefore accumulate less ice.

A pipe with a rough surface will however have a greater number of nucleation sites than a pipe with a smooth surface. Nucleation sites facilitate water nucleation. A greater number of nucleation sites would increase the accumulation of water and ice on a pipe surface [17].

It has been found by Jellinek [12] from a test done at -4.5 °C that ice has a greater adhesion force to stainless steel with a rough surface than stainless steel with a smoother surface. The roughness was varied five times and as the stainless steel became progressively smoother the adhesive strength of the ice decreased from approximately .598 MPa for stainless steel with a "Lathe Finish" to .067 MPa for stainless steel with "Bright Mirror Polish". It is unknown if this ice is the same type of ice that accumulates in fuel pipes. It is however expected that the ice that accumulated in fuel pipes may be similar because of the temperature and pressure that the tests were done.

Dependence of Ice Accumulation on Electric Fields

Application of an electric field will increase the rate of ice crystal growth [10]. Many of the electric fields that were shown to increase ice crystalization tested by Hobbs [10] are greater than may be expected on an aircraft. The effect of electric fields on a plane may be minor compared to the effect of other ice contributors.

Dependence of Ice Accumulation on Temperature

The rate at which ice accumulates in a fuel pipe depends on fuel temperature. The results from Boeing state that ice has a sticky consistency between -5 °C and -20 °C and has the highest level of stickyness at -12 °C [3]. The sticky ice in the Boeing report refers to ice particles that have nucleated heterogeneously elsewhere in the flow and then come in contact with pipe surfaces.

Temperature is also correlated with contact angle mentioned in section 1.2.7 and critical radius of nucleation.

The adhesion strength of ice varies with temperature. Gouni [9] determined the variation of adhesion strength of ice to type 304 stainless steel in a temperature range of -10 °C to -20 °C. It was found that the ice has an adhesive strength of about .77 MPa at -10 °C and increases almost linearly to 1.42 MPa at a temperature of -20 °C. This work confirms similar test data with stainless steel done by Jellinek [12].

Gouni [9] also showed that as the temperature of the ice decreased, the ice had a greater adhesive force to the stainless steel than a cohesive force to itself.

Dependence of Ice Accumulation on Rate of Shear

The rate of shear that is applied to ice that has accumulated in a pipe affects its growth. Jellinek [12] showed that for "mirror polished" stainless steel, the adhesive strength increased from 0.00726 MPa at a lower shear rate of $.53 \cdot 10^{-3}$ $\frac{cm}{sec}$ to 0.0706 MPa at a higher shear rate of $41 \cdot 10^{-2}$ $\frac{cm}{sec}$. If the type of ice used in this experiment was similar to the ice in aircraft fuel pipes, sudden changes in fuel flow would increase the adhesion of ice to the pipe. If this type of ice was the same as ice found in an aircraft fuel system, sudden changes in fuel flow would be less likely to take ice off of the surface than would prolonged changes in fuel flow.

Dependence of Ice Accumulation on Fuel Flow Turbulence

The rate of ice accumulation on a fuel pipe surface is dependent on the amount of turbulence in the flow. Turbulence mixes the fuel/H_2O mixture and increases the flux of water and ice to the pipe surface. At a constant Reynolds number, shear stress on the ice decreases as turbulence increases. The existence of turbulence may therefore increase the rate at which ice accumulates.

Ice accumulation may be accounted for from basic fluid flow principles. Reynolds number is a dimensionless quantity that ties flow velocity, pipe diameter and viscosity together. The relation is given by equation 1.3. In this relation, D is the pipe diameter, u is the flow velocity and ν is the kinematic viscosity.

As Reynolds number increases, mixing increases and thus there is a tendency for ice to accumulate. However, as Reynolds number increases, assuming constant viscosity, shear stress also increases and therefore ice accumulation would tend to decrease. These factors account for two competing contributors.

$$Re = \frac{Du}{\nu} \tag{1.3}$$

Fuel flow in commercial airliners is commonly measured in pounds per hour (PPH). With assumption of an appropriate viscosity (which may vary among different batches of fuel), an appropriate pipe diameter and conversion of PPH to meters/second with use of the fuels density, Reynolds numbers for commercial aircraft are approximately in the range 3000 to 13750. The lower limit of 3000 pertains more to smaller commercial aircraft and the upper limit of 13750 pertains more to larger commercial aircraft.

Dependence of Ice Accumulation on Cooling Rate

Nitsch [20] showed that the cooling rate, the rate at which something cools (temperature/time), and overheating temperature, the upper limit of temperature that the water is brought to before it cools again, affects the process of heterogeneous nucleation. The results showed that as rate of cooling increased, the temperature at which liquid tended to supercool also increased. They also showed that as overheating temperature increased the supercooling temperature decreased [20]. These effects are however expected to be small compared to the effects of material and surface properties.

Dependence of Ice Accumulation on Heat Transfer From the Fuel Pipe

The heat transfer through the pipe to the fuel affects the rate of ice accumulation. For water to nucleate and form ice, it has to overcome an energy barrier called "Gibbs free energy". If the pipe material is below the freezing point of the entrained water and the water is above it, the droplets may tend to collide with the pipe and almost instantaneously overcome the energy barrier required for nucleation. The heat transfer from the fuel can be modeled by usage of Fourier's law with the heat equation in cylindrical coordinates. These equations are solved with boundary conditions: $T(r_i) = T_i$ and $T(r_o) = T_o$ and the result is given by equation 1.4. In this equation, L is the length of the pipe, T_i is the inner pipe temperature, T_o is the outer pipe temperature, k is thermal conductivity of the pipe and r_o and r_i are the inner and outer pipe radaii, respectively. The temperature of the inside of the pipe is approximately the fuel temperature and the temperature of the outside of the pipe may be measured with a thermocouple or any other suitable temperature measurement device.

$$Q_r = \frac{2\pi Lk(T_i - T_o)}{ln(r_o/r_i)} \tag{1.4}$$

The convective heat transfer coefficient from the pipe may be calculated from the heat transfer rate. The relation is given by equation 1.5. In this equation, A is the surface area of the pipe, T_{env} is the air temperature that surrounds the pipe and T_o is the pipe surface temperature.

$$h = \frac{Q_r}{A(T_{env} - T_o)} \tag{1.5}$$

The heat transfer coefficient h may also be calculated from theory. If h results from forced convection, a correlation given by Fand and Keswani in equation 1.6 may be used. In this equation, C and m are constants that depend on the Reynolds number for the flow on the outside of the pipe. The constants are listed in table 1.2. The values D, Re_D, Pr, and k are the outside pipe diameter, the Reynolds number at D, the Prandlt Number, and the thermal conductivity of the outside fluid, respectively [17].

$$h_{forced} = \frac{C \cdot Re_D^m \cdot Pr^{\frac{1}{3}} \cdot k}{D} \tag{1.6}$$

Table 1.2: Fands Constants for Forced Convection [17]

Re_D	C	m
1-4	-	-
4-35	0.795	0.384
35-5000	0.583	0.471
5000-50000	0.148	0.633
50000-230000	0.0208	0.814

The main fuel tanks of an aircraft have a much smaller surface area to volume ratio than the fuel pipes. This means that if the surface of the fuel tanks and the surface of the fuel pipes are at the same cold temperature, and the aircraft fuel pipes are not insulated, the fuel in the pipes will tend to cool faster.

Dependence of Ice Accumulation on Fuel Contaminants

Contaminants such as dust may enter the fuel through vents or may be present in the fuel upon delivery. The results of [19] suggest that ice may require contaminants or a surface such as the pipe wall to nucleate (heterogeneously). The fuel alone was not shown to be a suitable nucleus for ice formation [19]. Contaminants that are delivered with the fuel such as metals, dust, or sulfur may be a significant cause of ice crystallization in fuel.

Transport to Pipe Surface

There are three properties that contribute to the transport of ice and water to the pipe surface. These contributors are bulk fluid motion, previously described in subsection 1.2.7, diffusive transport and buoyancy transport.

Turbulence is not an exact science and is more often described statistically. Turbulence aids in the transport of particles to the wall. Greater turbulence correlates with greater velocity fluctuations, with the assumption that the mean flow velocity remains constant. These velocity fluctuations would tend to move particles in the direction of the wall through turbulent diffusion. Velocity fluctuations alone are not able to bring the water or ice to the wall because fluctuations are zero there. Instead, when the ice or water comes close enough to the wall, its momentum or molecular forces bring it the rest of the way.

Diffusive transport of ice or water to the pipe wall can be described from the Bergeron process with consideration of partial pressures. Additionally, if the particles are assumed small enough they may be described by a diffusion law such as Ficks law. The overall effect of diffusive transport of ice or water to the pipe wall is small compared to convective transport except for cases with very low flow rates or regions close to the pipe surface.

The effect of buoyancy transport to the pipe surface may be described by consid-

eration of densities and Stokes drag. The density of water is 0.9998 $\frac{g}{cm^3}$ at 0 °C and the density of jet fuel is about .8 $\frac{g}{cm^3}$ [28]. Because the densities of fuel and water are within approximately 20% the transport due to buoyancy forces is considered small compared to convective transport.

The density of ice is approximately $0.9167\frac{g}{cm^3}$ at 0 °C which makes it even closer to fuels density of $.8\frac{g}{cm^3}$ [28]. The settling velocity of ice would be less than $2{\cdot}10^{-5}\frac{m}{s}$ and the effect of buoyancy transport may be considered negligible [6].

1.3 Objective

The objective of this study is to understand the process of ice accumulation in fuel pipes and then to suggest possible solutions to prevent its occurrence.

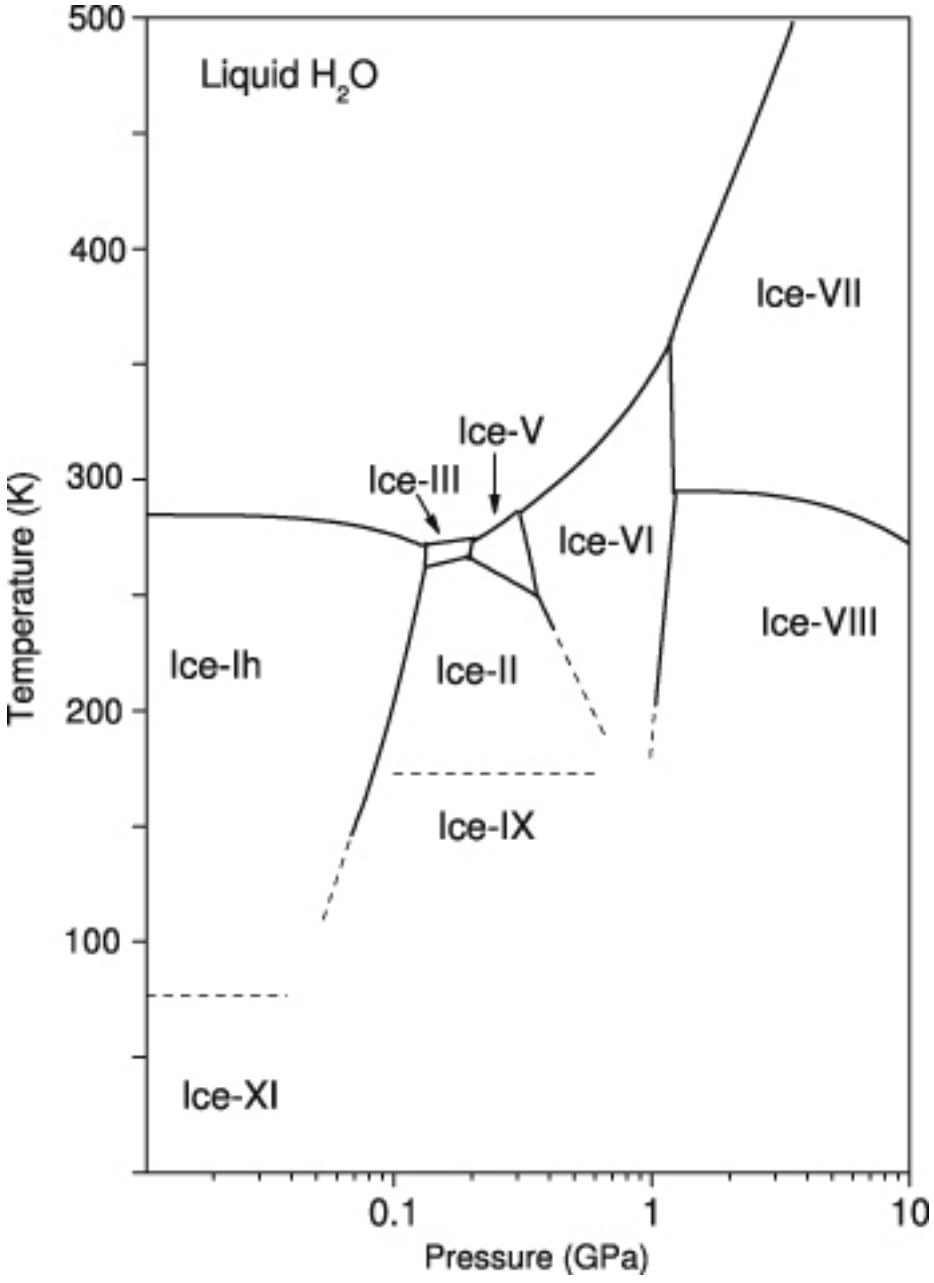

Figure 1.3: Ice Phases [21]

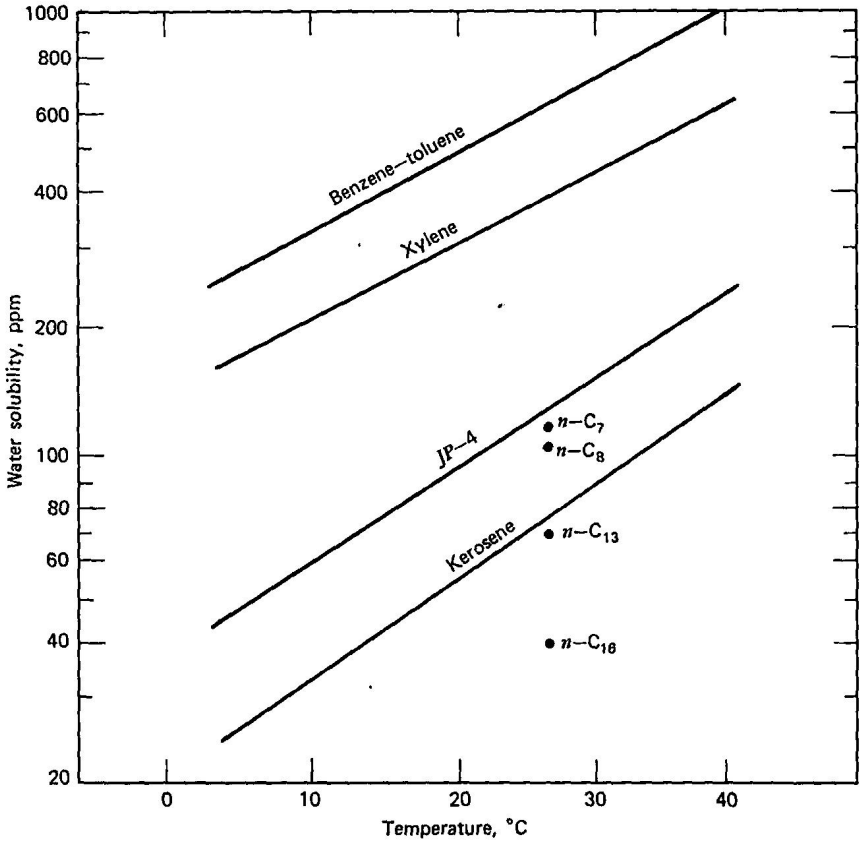

Figure 1.4: Variation of Water Solubility of Hydrocarbons with Temperature [13]

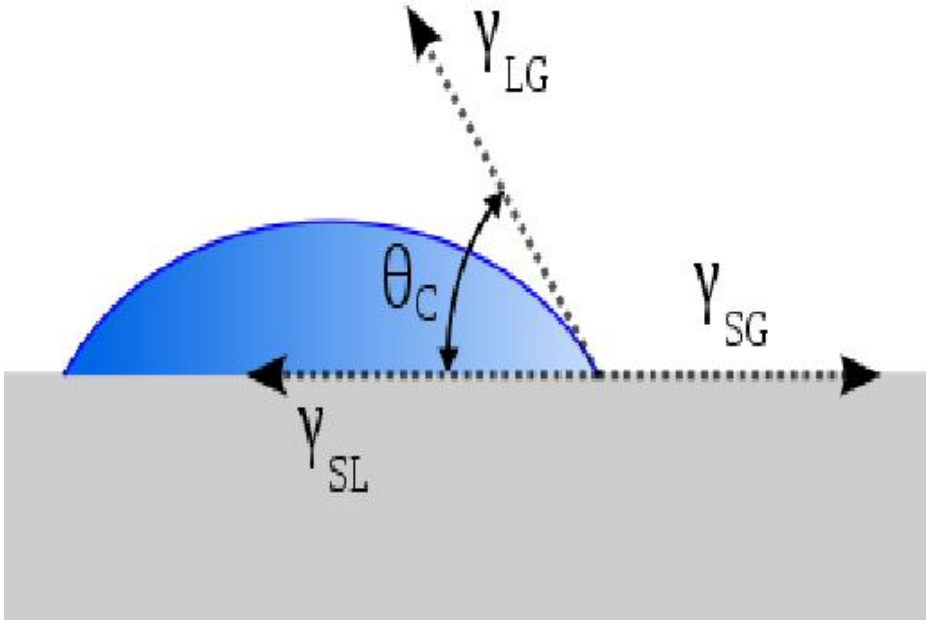

Figure 1.5: Illustration of Contact Angle [27]

2. Experimental Setup

This chapter describes the experimental setup for the fuel icing experiments of this study. The experiments took place in an altitude chamber and measurements were taken with pressure and temperature devices. Jet A-1 fuel was circulated with a 3/4 hp motor and gear pump through a pipe configuration with two removable test pipes. Each test pipe had an upstream and downstream pressure measurement port. Additionally, each test pipe had a downstream thermocouple. There were three thermocouples on the outside top of each test pipe. The test pipes were sometimes insulated and sometimes un-insulated while the remaining pipe network was almost always insulated. The flow loop had a flow orifice calibrated with a pressure transducer to measure flow rate. In a secondary flow loop was a 5 micron water separator (coalescer) and a 10 micron particle filter. The bottom of the main fuel tank had a metal tray for free water storage. The system had a high flow rate sump pump used for emulsification of the fuel and a sump valve for drainage of excess water and fuel samples. Figures 2.1 and 2.2 give a representation of the fuel system.

As each test took place, fuel leaked from various places. This fuel was collected with drip trays and put into a single container. After a sufficient amount of time (approximately 2 days), when any contaminants had time to settle, all but approximately $1''$ of this fuel was slowly pumped back into the system. The remainder was left for debris.

2.1 Altitude Chamber

The main facility that was used for tests was an altitude chamber (figure 2.3). The chamber was capable of a minimum of -60 °F and a pressure equivalent to an altitude of 40,000 feet. The fuel test loop was inside the chamber and after each test there was sufficient room for a person to enter and close the door to lock in cold air. This allowed more time to disassemble each test pipe and capture images.

2.2 Test Pipes

There were several pipe materials and geometric variations that were used with the test setup. Insulation was used on the pipes to control heat transfer and after each test the upstream and downstream pipe sections were photographed.

The pipes are shown in figure 2.4 and descriptions of them are as follows:

- Two schedule 40 type 304 stainless steel pipes were used. One of these pipes was $1''$ and the other was $3/4''$. Both of these pipes were of weld construction.
- A schedule 80 $1''$ Teflon® (PTFE) pipe was used for experiments.
- Two schedule 40 $1''$ T6 aluminum pipes were used for tests. One of the aluminum pipes was scratched (perpendicular to the flow direction) with 80 grit sand paper.
- A pipe section with a diameter increase and two pipe sections with bends were also used. The sections with the diameter increase and bends were aluminum. The radii of the bends were 1 $\frac{1}{4}''$ and 2 $\frac{1}{4}''$ and the ratio of diameters for the area increase was $1''/1.5''$

All of the test pipes were fitted with two pipe unions; one at the entrance and one at the exit and all of the straight test pipes were two feet in length (within half of an

inch).

There were two positions in the fuel system to put test pipes, a top position and a bottom position. The top position had greater exposure to the chamber fan and therefore had greater heat transfer. The 3/4″ pipe was always in the top position and the 1″ pipes were usually in the bottom position but were moved to the top for some tests (see figure 2.1). Upstream of each test pipe was an entrance region of about .635 meters (2 feet) to allow the flow to become fully developed.

The insulation that was sometimes used for the test pipes was polyurethane foam with a K-factor of .17. The insulation that was on the rest of the system pipes was fiberglass with a K-factor of .3.

Images of the inside of the test pipes were captured after each test at upstream and downstream locations. Initially, in earlier tests, images were deemed lower quality but later, they improved with use of an Everest VIT PLS 500 D video probe. The probe captured images in two positions, one position with the lens flush with the pipe entrance and the second with the lens approximately 2″ away. When it was time to capture images, the camera and test pipe were mounted into position and the images were taken as shown in Figures 2.5a and 2.5b.

2.3 Fuel

The main fuel tank held approximately 115 gallons of Jet A-1 fuel from the previous FAA tests done two years earlier. If the water concentration of the fuel was assumed to be 100 ppm at 21.5 °C when saturated then the 115 gallon fuel system would have about 43.5 mL of dissolved water.

From later tests it was observed that the fuel contained contaminants. The type and quantity of contaminants was not known and its analysis was saved for future work.

Viscosity

Because the viscosity of fuel depended on its composition and the composition was not a specified parameter (section 1.2.3), tests were necessary. Determination of the viscosity of the specific batch of Jet A-1 was done by experiments at various temperatures. The viscosity was found with the use of two glass viscometers to cover the full range of viscosities. The viscometer used for the temperature range 0 °C to 20.7 °C was a Cannon-Fenske Opaque viscometer. The viscometer used for the temperature of -11.7 °C was an Industrial Research Glassware LTD. Both viscometers were submersed in a temperature bath of anti-freeze and the time (in seconds) it took for the fuel to travel from one line of the viscometer to the next line of the viscometer was multiplied by a calibration constant. The result gave a kinematic viscosity with units of centistokes (cSt). The uncertainty of the Cannon-Fenske Opaque viscometer was listed as about 1% and the uncertainty of the Industrial Research Glassware LTD was not listed. This data was used to solve for a 3rd order polynomial to represent the viscosity, shown in figure 2.6. It may be noted that fuel viscosity does not necessarily follow a 3rd order polynomial but the equation was convenient for representation of all of the data points.

Fuel Samples and Emulsion Pump

At the bottom of the main fuel tank was a sump valve. This was used to drain water that accumulated in the tank over time. Once the water was flushed out of the sump, the valve was used to take fuel samples before and after each test. Water content data from the samples are not in this study but may be analyzed at a later time.

A high flow rate pump was connected to the main fuel tank sump. For tests in which it was desirable to increase the amount of emulsified water in the fuel, extra water was added to the sump and the pump was turned on. The pump was a Kinsler fuel injection pump with model number: MQ347 and is shown in figure 2.7.

2.4 Pressure Transducers and Flow Rate Measurement

The pressure transducer for the bottom 1″ test pipe was a 0″ to 4″ WCD (water column differential) GC-52 and the pressure transducer for the top 3/4″ pipe was a -20″ to 20″ WCD Dynisco transducer.

Both transducers were located outside of the chamber where the temperature remained constant at approximately 75 °F. The uncertainty of the 0″ to 4″ WCD GC-52 transducer was .5% full-scale. The uncertainty for the -20″ to 20″ WCD transducer was 1% full-scale.

The flow rate was measured with an orifice nozzle and another -20″ to 20″ WCD Dynisco pressure transducer. The nozzle was calibrated at 9 flow rates with a graduated bucket. A fourth degree polynomial fit of this calibration was used for measurements. The pressure transducer used for the flow nozzle had an uncertainty of 1% full-scale. The bucket used for flow rate calibration was a standard 5 gallon bucket and was calibrated with a 2 liter graduated cylinder with 20mL graduations. The maximum calibrated flow rate that resulted from the flow polynomial was .7536 liters/second.

2.5 Temperature

The temperature was measured with type T thermocouples at various locations within the chamber. These locations include: immediately downstream of each test pipe, at the top of the chamber, the outside of each test pipe at the entrance, middle, and exit (between the insulation and the outside pipe surface when insulation was used), and within the fuel tank.

The thermocouples on the outside of the pipes were “zip-tied” tightly to the pipes. The top and bottom pipes each had an Omega brand 1/16″ grounded thermocouple in the centers. The bottom pipe had a “home made” thermocouple at each end and

the top pipe had store bought 1/16″ thermocouples of unknown origin. Downstream of each test pipe were 1/8″ ungrounded Omega brand thermocouples. Finally, the thermocouple in the main fuel tank was 1/16″ and of unknown origin. Figure 2.2 shows the locations of the thermocouples.

At 0 °C the type T thermocouples had an uncertainty of .5 °C and the DAQ had an uncertainty of ± 1.1 °C. The accuracy of the thermocouple wires and DAQ system were verified with a type T thermocouple calibrator.

2.6 Measurement of Water in each Test Pipe after an Experiment

After each test the quantity of water that had collected in each test pipe was drained into a tray and its volume was measured. The water volume was determined by the measurement of its length in a calibrated 1/8″ tube. Calibration was done with 3 mL of water from a .2 mL increment graduated cylinder. The 3 mL volume of water equaled 54 17/32″ in the 1/8″ tube. The calibration assumed that the tube had a constant diameter. An image of the water measurement device is shown in figure 2.8.

To aid in the removal of ice and water from the inside of the pipe, warm fuel was sprayed or poured on the ice and water. A squeegee was sometimes also used to assist with ice and water removal.

2.7 Data Processing

After each test the recorded data was processed in MATLAB for determination of important flow quantities. The major flow quantities that were determined were Reynolds number and five pressure related parameters. The pressure parameters were: theoretical pressure drop, normalized pressure, CNPI (Characteristic Normalized Pressure Increase), pressure increase, and total pressure rise. Density and friction

factor were found for determination of the theoretical pressure drop. All data that resulted from a pressure transducer was filtered.

Reynolds Number

Reynolds number was an important parameter that was used for flow rate comparison in this study. The three parameters for determination of Reynolds number (equation 2.1) were used at each time step. The flow rate, given in *liters/sec* from the flow orifice (section 2.4), was converted to *m/sec* with the pipe diameter. The kinematic viscosity was determined at the fuel temperature with the viscosity polynomial. These two parameters with the pipe diameter were then used for Reynolds number.

$$Re = \frac{Du}{\nu} \tag{2.1}$$

The maximum calibrated flow rate of .7536 liters/second, at a fuel temperature of -10 °C, gave a maximum calibrated Reynolds number for the $3/4''$ pipe of 14729 and a maximum calibrated Reynolds number for the $1''$ pipe of 11570.

Friction Factor

The friction factor was determined by iteration at each time step of each test. In the Colebrook equation (equation 1.2), the roughness height e was set to a constant value of $.015 \cdot 10^{-3}$ for the stainless steel pipes, the diameter D was set in accordance to the pipe that was tested, and Reynolds number was determined as described previously.

Density

The density of Jet A-1 fuel was assumed to be $810 \frac{kg}{m^3}$ at 15 °C and the coefficient of thermal expansion was assumed to be .00097/°C. A linear equation was constructed for determination of the density of Jet A-1 at other temperatures. Equation 2.2

presents this relationship. In this equation ρ_{JetA-1} is the new density of the fuel at the new temperature, T, and β is the coefficient of thermal expansion.

$$\rho_{JetA-1} = \frac{810}{1 + \beta(T - 15)} \tag{2.2}$$

Temperature dependent density was determined at each time instance of the flow from equation 2.2.

Pressure

Fuel flow restriction increased with ice accumulation which allowed the accumulation to be measured with differential pressure measurements.

At each time step in the test, the actual pressure drop given by the pressure transducers was divided by the theoretical initial pressure and the fraction was used to quantify ice growth.

The slope of this normalized pressure drop was then used to determine a CNPI (characteristic normalized pressure increase) which was the slope of the normalized pressure divided by the pipe length with units of $\frac{Pa_{actual}}{Pa_{initial} \cdot m \cdot hr}$. The portion of the normalized pressure plots that were used to determine the slope was arbitrary. Points were generally picked where the *slope* of the normalized pressure increase curve was a maximum and was approximately constant for about an hour.

A "pressure increase" parameter was determined from the slope of the *actual* pressure plot. It was determined in a similar manner to the CNPI but from the slope of *experimental pressure plots* instead of the *normalized pressure plots*.

A "total pressure rise" was also determined from the actual pressure plot by the subtraction of the initial pressure of each test from the greatest pressure of each test. The initial pressure and greatest pressure were determined by human selection of two points on the pressure plots.

The theoretical initial pressure drop across each pipe section was determined by

equation 1.1. In this equation density, velocity and friction factor were determined with the previous calculations. Δz was zero, gravity was 9.8 $\frac{m}{sec^2}$, and L and D were determined for each individual pipe. The diameter that was used for the $3/4''$ stainless steel pipe was 2.09 cm and the diameter that was used for the $1''$ stainless steel pipe was 2.66 cm. In the equation for the theoretical pressure drop the diameters were assumed constant throughout the tests even though they may have varied as ice accumulated.

Pressure data was filtered after each test with MATLAB's filter function which found a running average of the data input [18]. The filter size for each plot that was filtered is shown on the figures.

Other Parameters

Two other parameters that were determined in MATLAB after each test were the initial fuel temperature and the test length. The initial fuel temperature was the average of the first 10 temperature data points and the "test length" was the amount of time from when the constant "test temperature" was achieved to the end of the test.

Data Collection

All devices were wired to an Iotech data acquisition board with an uncertainty of .015% of the voltage input and then to a computer where readings were recorded once every 1-2 seconds. The software used for data collection was made at the FAA with visual basic.

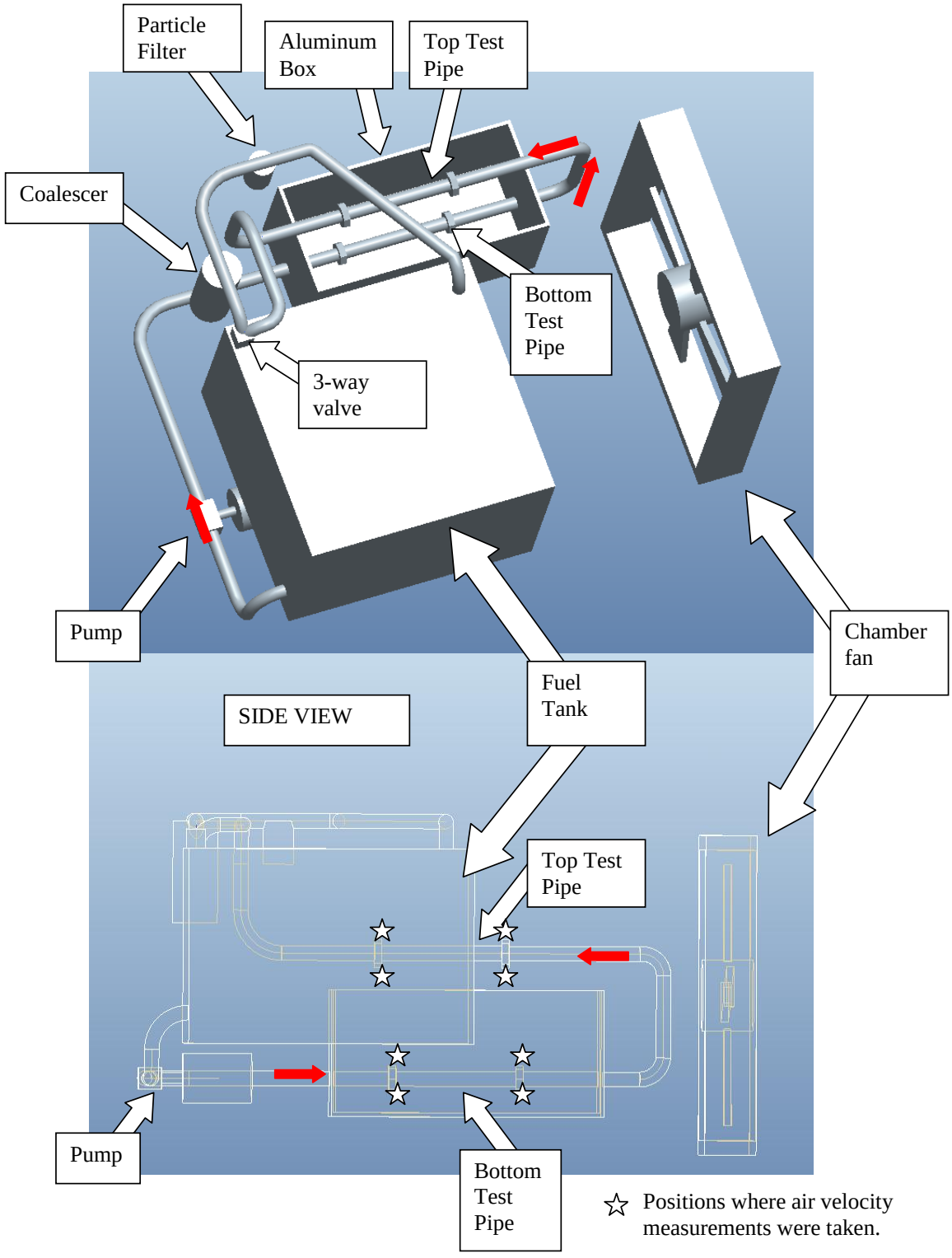

Figure 2.1: CAD Diagram of Experimental Setup

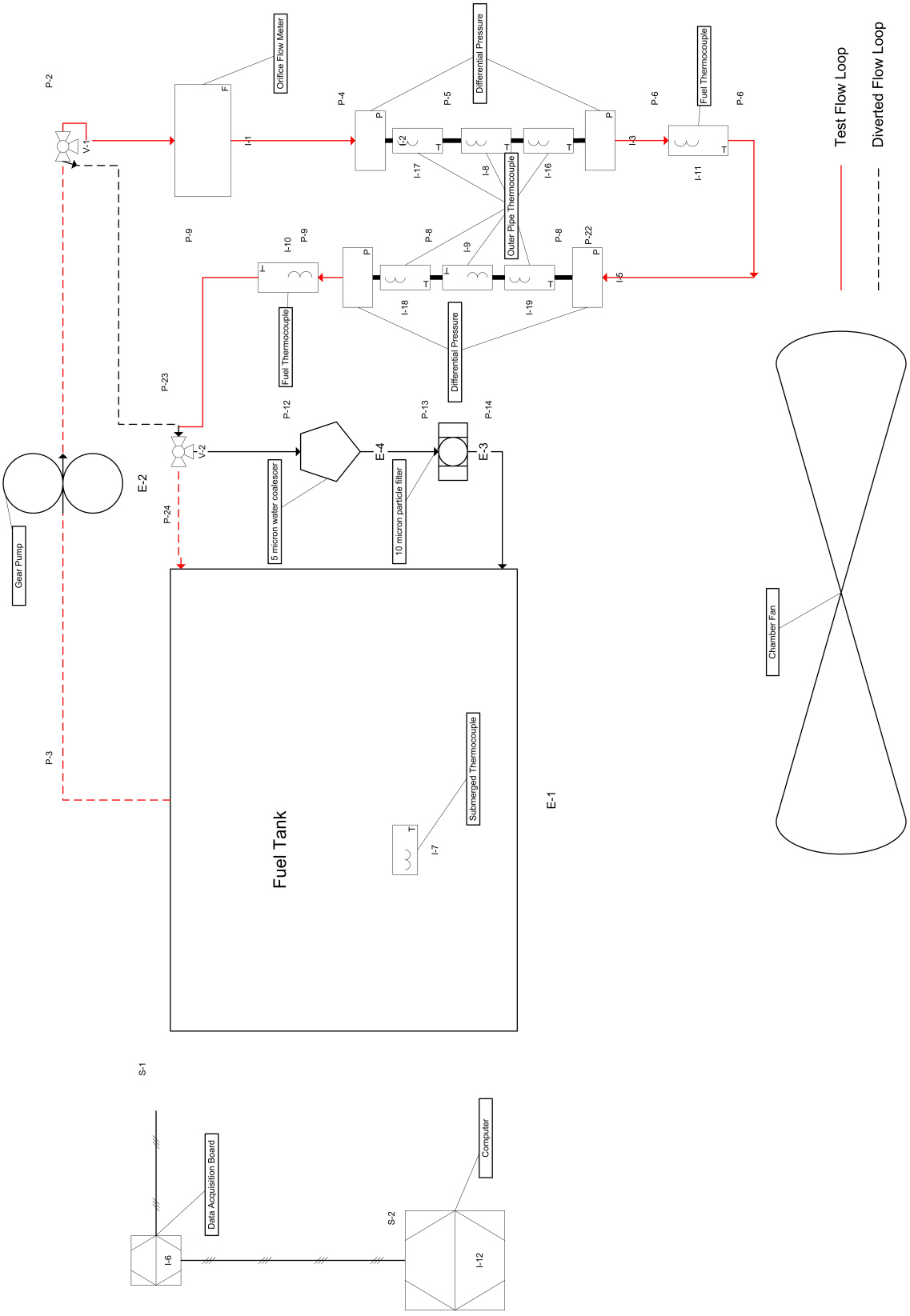

Figure 2.2: Block Diagram of Experimental Setup

Figure 2.3: Altitude Chamber

Figure 2.4: Insulation and Test Pipes. From Left to Right: Polyurethane Insulation, 3/4″ Stainless Steel, 1″ Stainless Steel, 1″ Teflon®, 1″/1.5″ Area Change, Scratched Aluminum, Aluminum

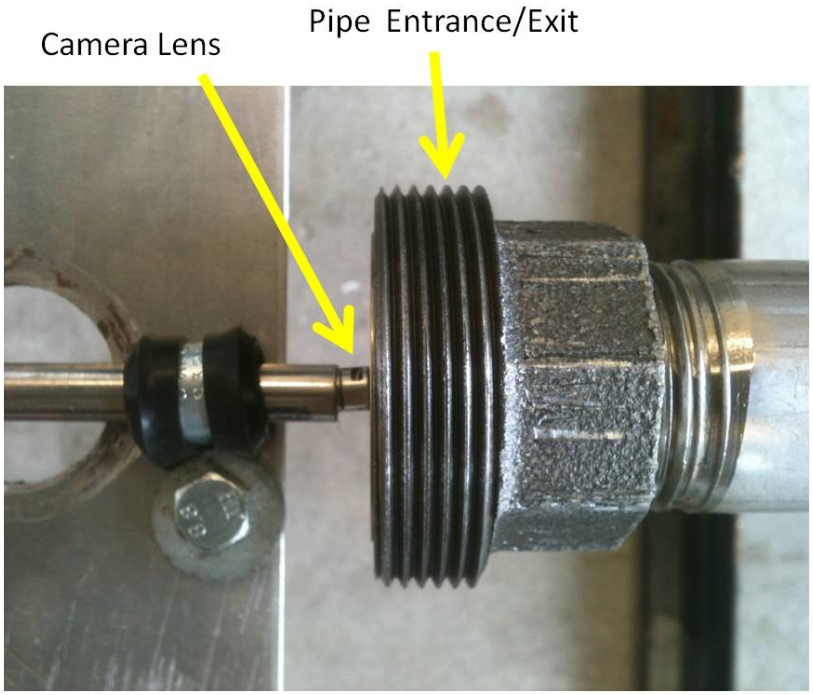

(a) Close-Up

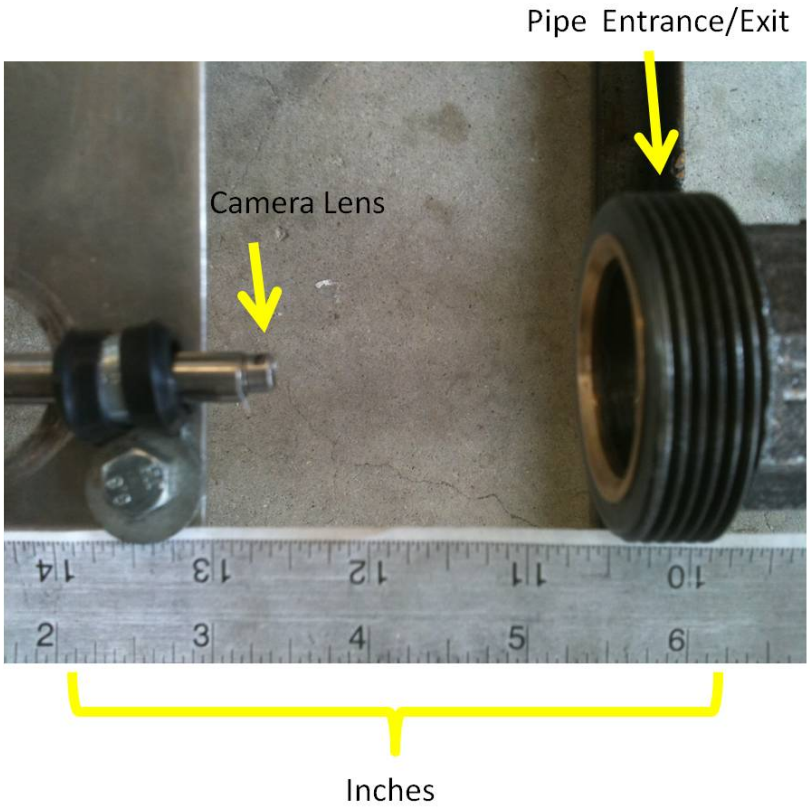

(b) Further Away

Figure 2.5: Camera Positions for Ice Images

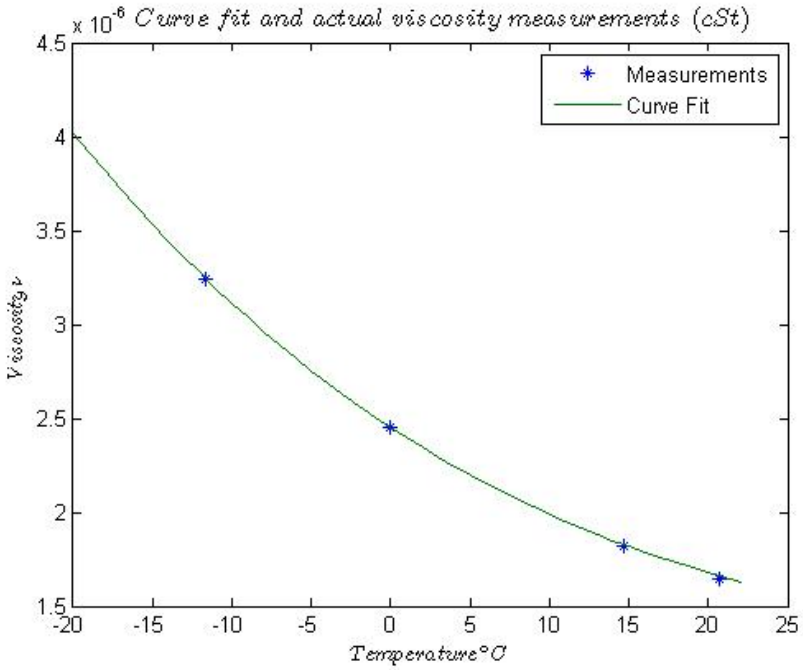

Figure 2.6: Fuel Viscosity

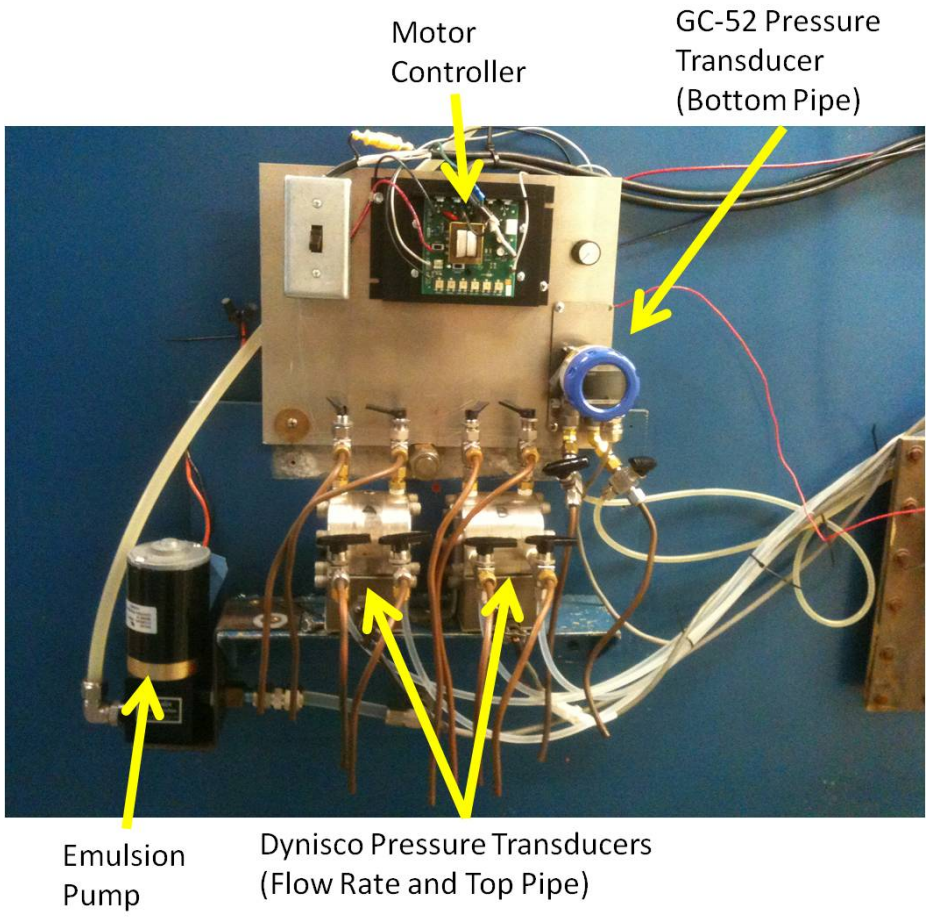

Figure 2.7: Pressure Transducers, Emulsion Pump, and Motor Controller

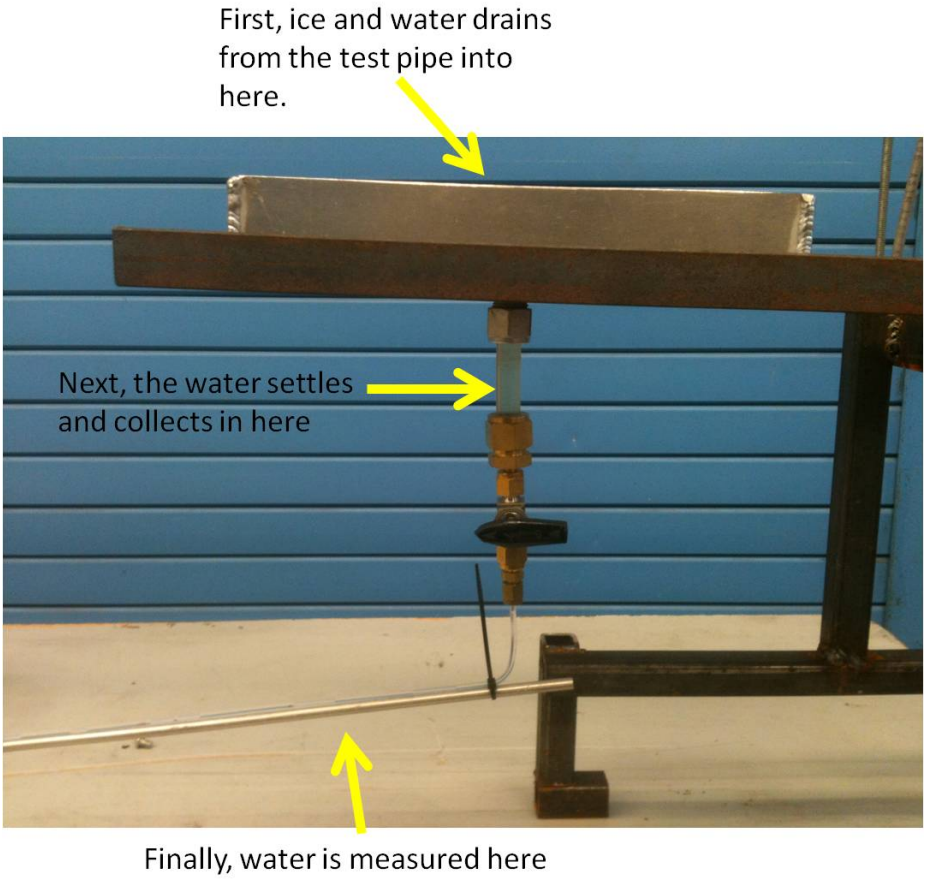

Figure 2.8: Apparatus for Water/Ice Volume Measurement

3. Experiments

This study was broken into two parts. First were initial tests, which would help in the attainment of a fundamental knowledge of why ice accumulated. These tests included the variation of pipe configurations and initial conditions. Once a firm fundamental knowledge was attained, specific initial conditions from these tests were selected for further analysis of temperature and flow rate variation. The initial tests are called "stage I" and the later tests are called "stage II".

3.1 Stage I

Initially, it was of interest to explore the effect of test conditions on ice accumulation. It was well known that the phenomena happened but it had not been extensively reproduced for test conditions identical to those experienced in flight. Stage I tests were performed in stages as shown in table 3.1. First, tests were performed that included the variation of initial conditions within the test pipes. Later when knowledge of the effect of these initial conditions was attained, the initial condition of the fuel was varied. Pipe geometry, pipe material, heat transfer from the pipe (insulation or no insulation) and pipe surface properties were also varied in stage I. The amount of contaminants in stage I tests remained approximately constant except for a negligible amount that left with the ice when it was melted at the end of each test.

All of the initial tests were carried out as described in the experimental procedure section unless stated otherwise. The test pipes had insulation in all of the stage I tests

unless stated otherwise. The remainder of the flow system did not have insulation.

Table 3.1: Stage I Test Conditions

3.1.2	Variation of Test Pipe Initial Conditions
3.1.3	Variation of Fuel Water Content
3.1.4	Variation of Pipe Material and Surface Properties
3.1.5	Variation of Pipe Geometry
3.1.6	Heat Flux Across the Pipe
3.1.7	Other Observations

3.1.1 Experimental Procedure

Stage I experiments were less restricted to certain preparation procedures. The procedures varied and were dependent on each individual test. If flow was not in the test pipes until the test temperature was reached, then the flow traveled through the diverted portion of the flow loop initially (shown in figure 2.2). In each test, the desired flow rate was first set and the desired flow loop was set. The chamber was then cooled to -60 °C. Once the cold chamber cooled the fuel to the desired test temperature, the chamber was warmed to the test temperature. Ice was allowed to collect for a variable amount of time. After this time, the chamber was opened and photos were taken of the test pipes.

When comparative tests were done, the same flow rate, test temperature and initial conditions were used. The initial temperature of the fuel varied from about 16 °C to 23 °C. Stage I tests did not have the tray of water at the bottom of the fuel tank, but rather had water directly in the sump of the main fuel tank.

3.1.2 Variation of Test Pipe Initial Conditions

There were four primary initial conditions that were varied in the test pipe. The first initial condition was fuel flow through the test pipe as the system cooled to the desired test temperature. This initial condition may be most realistic and would

represent a plane in flight. Next, stationary fuel was stored in the test pipe as the system cooled. This initial condition would represent a plane on the ground with a low flow rate. Later, stagnant dry air was stored in the test pipe as the fuel cooled to the test temperature. This condition alone may not relate to a service condition in an aircraft but was useful for comparison with the last initial condition. Lastly, about half of the test pipe was sprayed with water and the rest was left dry. The air and water (which had turned to ice) remained in the test pipe until the system reached the test temperature. This condition would represent a case in which water had accumulated in the fuel pipes over time and remained stuck, not able to pass downstream.

Table 3.2: Test Pipe Initial Conditions

#1	Fuel Flow Through the Test Pipe as the Fuel Cooled
#2	Quiescent Fuel in the Test Pipe as it was Cooled
#3	Dry Air in the Test Pipe as the Fuel Cooled
#4	Water Droplets and Air in the Test Pipe as the Fuel Cooled

Results: Test Pipe Initial Condition

The results of the initial condition tests are presented qualitatively in figures.

Pipe Initial Condition 1

The first condition was fuel flow through an insulated test pipe as it cooled. Figure 3.1a shows a qualitative image of the ice accumulation.

Pipe Initial Condition 2

Next, quiescent fuel was stored in the test pipe as the system cooled. Flow through the test pipe began once the desired test temperature was reached. Figure 3.1b shows qualitatively how the ice accumulated. For this test, a small portion of the test pipe

contained air initially. It is notable that more ice accumulated where this air was present than where the stagnated fuel was present.

Pipe Initial Condition 3

Later, the pipe was allowed to remain outside of the flow loop until it had become thoroughly dry of fuel and water. It was then placed into the flow loop and remained dry until the desired test temperature was reached. Once this temperature was reached, flow passed through the test pipe. Figure 3.1c gives a qualitative image of the pipe after the test.

Pipe Initial Condition 4

Next, about half (in the direction along the pipe length) of the test pipe was preconditioned with water and the other half remained dry. Fuel was not allowed to flow through the test pipe until the system had reached the desired test temperature. Figures 3.1d and 3.1e show before and after images of ice collection in the half of the pipe that was sprayed with water. The half that was not sprayed with water was similar to the previous case (Pipe initial condition 3) which had air alone present initially.

Discussion: Test Pipe Initial Condition

From the results of these initial conditions, several observations were made. It was shown that the two conditions that caused the most amount of ice to accumulate were the condition which had water injected into the pipe initially (initial condition 4) and the condition that had fuel flow through the test pipe as the main fuel tank was cooled (initial condition 1).

The conditions with water injected initially into the test pipe (initial condition 4) and with dry air initially in the test pipe (initial condition 3) are identical except for

the addition of initial water in case 4. The pipe with initial condition 4 (extra water in the test pipe) accumulated more additional ice than condition 3 (dry air alone in the test pipe). Additionally, ice that it did collect corresponded to the position where the water was initially injected. The other side of the pipe in case 4 that was not preconditioned with water had a lack of additional ice accumulation, similar to case 3. It was therefore shown that a layer of harder brittle type of ice present on the test pipe before the fuel reached sub-zero temperature promoted ice accumulation.

This suggested that the larger amount of ice that accumulated in initial condition 1 was because a layer of hard ice accumulated first as the pipe was cooled. This is likely because some of the entrained water that had separated from the fuel collided with the pipe and froze to create the layer of harder ice.

The remainder of the entrained water could have then frozen heterogeneously when the temperature dropped sufficiently, and formed entrained ice. This entrained ice may have made up the layer of soft ice that was observed to coat the harder ice.

Initial condition 2 showed that the quiescent air at the upper portion of the pipe which would have been saturated with water because the fuel was saturated, contributed more to ice accumulation than the quiescent fuel. The humidity in the air may have collected on the cold pipe and frozen. This could have created a layer of harder ice for the subsequent soft ice to collect on.

3.1.3 Variation of Fuel Water Content

The initial water content of the fuel was varied. The fuel in commercial aircraft may not reach supersaturated conditions at temperatures of 21.5 °C often, but it was of interest to observe the effect of extra emulsified water in the fuel. Two tests were performed: one near the saturation limit and one that was supersaturated.

Results: Fuel Initial Condition

Initial condition 1 (fuel flow as the system cooled) was used for the initial entrained water content variation. Extra water was introduced into the main tank and the fuel was supersaturated with the high flow rate sump pump. A qualitative comparison is given in figures 3.2a and 3.2b for the case of saturated and supersaturated fuel flow respectively.

Discussion: Fuel Initial Condition

As may be expected, the fuel that had more water also shed more water. This result could be further extended to give a qualitative comparison of fuels with different saturated initial temperatures. A fuel that is saturated at a higher initial temperature would have more dissolved water and would be expected to shed more water.

It is not known how much extra water was emulsified in the fuel. The reason that the difference between the two images is not great may be because some of the emulsified water had time to settle, as described in 1.2.5.

3.1.4 Variation of Pipe Material and Surface Properties

Three materials were tested to determine their effect on ice accumulation. These materials were: PTFE Teflon®, type 304 stainless steel, and 6061 T6 aluminum.

To test the effect of pipe roughness, an additional 6061 T6 aluminum pipe was scratched on the inside with 80 grit sandpaper.

Results: Pipe Material and Surface Properties

In the first test, Teflon® and stainless steel were tested at equal flow conditions. This provided a qualitative comparison of ice accumulation behavior. They were done simultaneously at the top and bottom flow positions (figure 2.1). Teflon® was at the

top. Figures 3.3a and 3.3b show the results of this test. In the image of Teflon®, the large chunk of ice is stuck to the union and a loose piece of Teflon® tape, and not the Teflon® pipe. The average Reynolds number for this test was 2023 and the average temperature was -9.5 °C.

In the next comparative test, stainless steel and rough aluminum were tested simultaneously. Scratched aluminum was at the top position of the flow loop. Results are shown in figures 3.4a and 3.4b. The average Reynolds number for this test was 5975 and the average temperature was -9.5 °C.

Discussion: Pipe Material and Surface Properties

The first test showed qualitatively that stainless steel accumulated more ice than Teflon® at these flow conditions. This was to be expected because of the relatively high hydrophobic nature of Teflon® in comparison to stainless steel and from the ice adhesion tests performed by [15]. Results from later tests indicated that the top pipe had a greater tendency to accumulate ice. Even taking this into account, Teflon® still accumulated less ice.

The second test with stainless steel and rough aluminum showed that stainless steel visually accumulated more ice on the upstream section than rough aluminum. It is not know what the water content in each pipe was at the end of the test. It could have been that the rough aluminum had a smaller contact angle than stainless steel and had a thin layer of ice with more water than is apparent from the image. The contact angle for stainless steel is typically greater than the contact angle for *smooth* aluminum. According to Wenzel's model [30] the surface roughness on the aluminum would decrease the contact angle further.

3.1.5 Variation of Pipe Geometry

Large and small radius pipe bends and area changes were tested. The large pipe bend had a radius of approximately 2 $\frac{1}{4}$ inches and the small pipe bend had a radius of approximately 1 $\frac{1}{4}$ inches.

Results: Pipe Geometry

Tests with bends and area changes were carried out. The pipes for this case were not insulated. Results of the pipe bends are shown in figures 3.5a and 3.5b. Images for the area change were not as clear but a qualitative description is presented.

Discussion: Pipe Geometry

Results of these tests showed that gradual pipe bends (figure 3.5a) and less gradual pipe bends (figure 3.5b) had very homogeneous downstream ice accumulation, both without a preferred growth area. This could be because the flow was already at a great enough turbulence level and the bend turbulence contribution was insignificant. It is not known how the pipe bends effected ice accumulation further downstream.

After a pipe diameter increase, there was a less ice dense area followed by a more ice dense area. The difference with ice accumulation from the area change was subtle, but may be explained as follows: immediately downstream of the diameter increase would be a recirculation eddy. This area of pipe would not come into contact with as much water and ice because the eddy itself has the potential to re-circulate the same volume of fuel; it has a greater residence time. Further downstream, the fuel is more chaotic and the turbulent mixing would tend to be greater.

Over a large amount of time however, the recirculation zone immediately downstream of the pipe diameter increase could have had the potential to build up more ice than the region further downstream because the shear stress was lower.

This test at these flow conditions did not give conclusive results for the effect of a pipe diameter *decrease* on ice accumulation. The entrance region to the straight pipe tests however behave as a diameter reduction and give a more qualitative result for the diameter reduction effect.

3.1.6 Heat Flux Across the Pipe

This subsection deals with a comparative analysis of the effect of insulation on the pipe as it is cooled. In stage II of this study this phenomena is explored quantitatively and in more detail with stainless steel. The results of this subsection are for scratched (with 80 grit sand paper) T6 aluminum and PTFE Teflon®.

Results: Heat Flux Across the Pipe

Figures 3.6a and 3.6b gave the results of a single rough aluminum test pipe with the upstream portion insulated, and the downstream portion un-insulated. The approximate Reynolds number for this test was 6034 and the average temperature was -9 °C. Figures 3.7a and 3.7b show Teflon® with the upstream insulated and the downstream not insulated.

Discussion: Heat Flux Across the Pipe

These images showed that ice accumulation was greater for the portion of the test pipe that was not insulated. This could be predicted because the colder test pipe would be a greater energy sink to the fuel and would tend to cause the fuels' entrained water to stick and freeze upon contact. Teflon® has a larger contact angle than other materials and would seem less likely to have any ice accumulation. It did however had a notable amount with the un-insulated condition.

The portion of Teflon® that was not insulated was shown to lack ice accumulation in an area of about a half of an inch from the exit of the pipe. This may be due to

the entrance and exit effects that are further discussed in 3.1.7.

3.1.7 Other Observations

There were other observations that were made while conducting stage I tests. Observations were made about the condition of the ice that was found in the pipe. There was also evidence that showed the behavior of the fuel system as multiple tests were run sequentially. There was indication of the freeze temperature of at least one of the types of ice that accumulated.

Ice had a tendency to accumulate on the schedule 40 pipe welds more than other areas of the pipe. A test with an upside-down pipe orientation was done to further investigate this occurrence.

Results: Type of Ice Found

After images were taken for one particular test, the ice was examined closely. A layer of movable softer ice was found on top of a layer of harder brittle ice.

Discussion: Type of Ice Found

The soft type of ice was consistent with what Boeing [3] found in their research and with initial condition 4 of this study. The soft ice and the brittle ice that was found may be explained by the physics of the system. As the fuel cools, dissolved water becomes entrained water. When the fuel is above the freeze point of the water (which may be different than 0 °C because of the fuel) and the test pipe is below the freeze point of the water, the entrained water may tend to stick and freeze to the colder pipe surface. This explains the formation of the hard ice layer. As time progressed and the fuel became cold enough, some of the remainder of the entrained water froze (heterogeneously) and became the soft ice. The soft ice then had a tendency to stick to the layer of hard ice and itself. The accumulation of the softer ice was supported

by pipe pressure data and was shown in greater detail in stage II of this study.

The soft ice seemed to exist in individual soft clumps as is evident from the picture. Light surface pressure on the ice would cause it to break apart.

Results: Sequentially Run Tests

Observations were made for the accumulation of water in the system over time. When tests were performed sequentially and the Reynolds number for the 1″ pipe was not brought above 6000, the amount of ice shown in the images increased as the number of experiments increased. Additionally, when the flow rate was turned up for the first time to a Reynolds number of about 12000 for the filter process at 21.5°C, several mL of water from the fuel pipes were observed to accumulate in the coalescer.

Discussion: Sequentially Run Tests

As tests progressed, the amount of water in the pipes increased. It is likely that much of the water collected in low velocity or "dead areas" of the system. This gave evidence that the adhesion force of the water droplets was too great to be overcome by the shear stress of the flow. It was for this reason that the fuel was filtered at a higher velocity for later tests.

Results: Ice Accumulation on Welds

Ice had a tendency to accumulate more on the test pipe welds than on rest of the test pipe. Results from a test pipe that was rotated 180 degrees showed that the ice still preferred the welds (figure 3.8).

Discussion: Ice Accumulation on Welds

This test showed that the affinity for ice to accumulate on the welds was independent of pipe orientation; it was independent of heat transfer to the pipe, and any other

non-symmetric fluid flow that could be in the system. It is however expected that other effects, such as heat transfer, that promote ice accumulation could enhance accumulation on the weld. From observation, it appeared that more of the harder ice and softer ice accumulated on the welds then elsewhere.

Results and Discussion: Freeze Temperature Indication

When the flow rate was turned up after tests, the motor controller would not allow the motor to return to its full potential velocity until the fuel temperature reached about zero Celsius. This indicated that the motor required too much power to reach its set rotational velocity. The motor returned to normal operation once the temperature rose above zero Celsius. It was logical to conclude that ice had caused the obstruction and had melted at about 0 °C. It is unknown if this was the harder or softer type of ice that caused the obstruction or where it was in the pipe system. This showed that for one or both of the types of ice found, the fuel contributed within the thermocouple accuracy to a change in freeze temperature.

Results and Discussion: Entrance and Exit Effects

The entrances and exits to the test pipes were shown to accumulate ice differently than the centers of the test pipes (figures 3.2, 3.3, 3.4a, 3.11, etc..)

The entrance and exit to each test pipe accumulated ice differently. The entrance and exit to the 1″ stainless steel bottom pipe is shown in figure 3.9. Graphical temperature results are also presented to show (figure 3.10) the variation in temperature from the thermocouples along the outside of the pipe.

At the entrance and exit to each pipe there were three major factors that contributed to ice accumulation. The lip at the entrance created turbulence. The turbulence effected the *shear stress* on the ice and the *flux of water and ice* to the pipe wall.

The third and possibly greatest effect at the entrance and exit was from the *colder temperature of the pipe unions*. The unions were not insulated and the aluminum box (figure 2.1) that the bottom pipe was closely attached to may have behaved as an energy sink.

Temperature Variation on the Outside of the Pipe

The outside of the pipe had three evenly distributed thermocouples. The temperature difference between these thermocouples and the fuel temperature was approximately constant for the period of time that the fuel was being cooled. Figure 3.10 shows the three outside thermocouples and the fuel temperature thermocouple from a typical test.

3.2 Stage II

As stage I tests progressed, a broader viewpoint was attained for the physical and environmental characteristics that contributed the most to ice accumulation. There were many test properties that could be varied. Two parameters that aircraft have less control of are temperature and flow rate. An aircraft can control heat transfer from the pipe with pipe insulation, the initial water content of the fuel may become more strictly controlled, and the pipe material may be varied but the flow rate and temperature of the fuel are more likely to continue to vary throughout the duration of the flight.

First, repeatability tests were performed. Next, the temperature, Reynolds number, and insulation of the pipe were varied according to table 3.3. This range of Reynolds numbers spans what is commonly encountered in large aircraft as mentioned in 1.2.7. This temperature variation covers what was previously observed as the sticky region for ice to accumulate [3]. Finally, the effect of a decrease in fuel contamination was explored. Dates are shown in table 3.3 and the time stamps of the images for ease of reference.

Pressure differential in the pipe was measured directly and was normalized by the expected theoretical pressure differential across the pipe. The differential pressure data was further quantified by a "normalized characteristic pressure increase" (chapter 2.7).

Reynolds number was varied first. After Reynolds number was varied, the fuel was filtered aggressively to reduce contamination, and the temperature was varied.

To establish the accuracy and confidence of the experiments, repeatability tests were performed. These repeatability tests were done for the middle section of the "X" in table 3.3.

Table 3.3: Test Matrix

Reynolds Number	-7.4 °C	-11 °C	-19.4 °C
3150		(3/19/12), 3/28/12	
4000			
6568	(4/13/12)*, 4/05/12**	(3/12/12), 3/22/12 (3/15/12), 3/26/12	(4/16/12)*, 4/02/12*
8362		(4/11/12)*, 4/09/12*	
10150		3/30/12	
12922			

() These tests had insulation.

* These tests had less contamination then other tests

** This test had less contamination and the pipe was oriented up-side-down

3.2.1 Experimental Procedure

Each test followed a list of procedures. At least 12 hours before each test, the fuel was allowed to warm to 21.5 °C. Once the fuel reached this temperature, it was filtered for water for several hours. For at least 30 minutes of this time, the fuel was circulated through the filters at an above average flow rate to clear water out of the pipes.

Later (at least 12 hours) the test was ready to commence. Immediately before each test a fuel sample was taken from the sump valve (after it was flushed for any accumulated water). The pump was turned on to the desired flow rate, and fuel passed through the test pipes ("Test Flow Loop" in figure 2.2). The chamber was then cooled to -50 °F. When the chamber air temperature brought the fuel temperature to the desired test temperature, the chamber was warmed to equal this temperature. The temperature controller was then turned off and the fuel was allowed to circulate for approximately three and a half hours. At the end of this time access was made into the chamber and the test pipes were photographed one by one. After the photographs were taken, and before the ice had time to melt, the pipes were set up over the water

collection tray and their water contents were measured. The chamber would then be turned back on to 90 °F to warm the fuel for the next test.

3.2.2 Repeatability

To determine the accuracy of the quantitative temperature and Reynolds number variation, it was necessary to perform repeatability tests. There were three parameters used to quantify ice accumulation that were used to determine the repeatability. These were the images (upstream and downstream), the pressure data and the water collected from the test pipes after each test. Reynolds number, test fuel temperature, and initial fuel temperature were also observed for repeatability.

Results: Repeatability

The repeatability images for the *1″ insulated* pipe are shown in figures 3.11a and 3.11b. The repeatability images for the *1″ un-insulated* pipe are shown in figures 3.12a and 3.12b. The repeatability images for the *3/4″ un-insulated* case are shown in figures 3.13a and 3.13b. Each set of repeatability images are followed by normalized pressure plots.

The value for the CNPI for the first and second tests with the un-insulated 3/4″ pipe were .709 and .664 respectively. Finally, the water collected after each test is shown in tables 3.4 and 3.5.

The normalized pressure increase for an additional repeatability case is shown in figure 3.14.

Discussion: Repeatability

The images showed repeatability, partially in the quantity of ice observed and strongly in the placement of the ice. It was shown that certain areas of the pipe seemed to be more prone to collect ice. The pressure data also showed repeatability. Values for

	3/12/2012	3/15/2012	3/19/2012	3/22/2012	3/26/2012	3/28/2012	3/30/2012	4/2/2012*	4/5/2012*	4/9/2012*	4/11/2012*	4/13/2012*	4/16/2012*
Average Reynolds Number	6494	6419	3153	6689	6609	3151	10151	6668	6087	6388	6485	6454	6657
Average Fuel Temperature	-11	-10.8	-10.8	-9.86	-10.2	-10.6	-10.7	-19.3	-7.4	-11.2	-11.1	-7.02	-19.5
Average Rate of Cooling ($\frac{^\circ C}{hour}$)	9.5	10.65	9.3	8.967	9.065	9.991	9.57	8.709	10.59	9.778	8.32	10.13	8.7
Initial Fuel Temperature	21.74	23.15	21.85	22.33	22.3	22.79	21.06	22.97	22	22.23	22.43	20.78	22.16
H_2O Collected from Pipe after Test (mL)	0.079	0.101	0.201	0.101	0.132	0.168	0.346	0.101	0.019	0.105			0.162
Test Duration (hrs.)	3.204	3.371	3.153	3.273	3.365	3.29	3.26	3.172	3.303	3.269	3.3	3.24	3.17
Total Pressure Rise (Pa)	29.88	26.43	27.84	58.48	47.89	26.2	62.37	2.46	9.05	42.1	45.64	-6.4	34.7
Normalized Characteristic Pressure Increase	0.186	0.09	0.356	0.316	0.319	0.402	0.056	-0.02	0.028	0.139	0.162	-0.06	0.045
Rate of Pressure Increase ($\frac{Pa}{m \cdot hr}$)	35.96	17.83	19.38	59.69	61.88	12.34	31.9	1.46	2.586	24.54	33.19	-7.49	36.04
Average Flow Rate ($\frac{L}{sec}$)	0.433	0.427	0.21	0.434	0.433	0.208	0.672	0.55	0.372	0.429	0.435	0.391	0.552
Average Viscosity (cSt) ($\cdot 10^6$)	3.189	3.179	3.179	3.102	3.129	3.16	3.167	3.957	2.918	3.211	3.204	2.892	3.968

Table 3.4: Stainless Steel, 1″, Bottom Position (* denotes less contamination)

	3/12/2012	3/15/2012	3/19/2012	3/22/2012	3/26/2012	3/28/2012	3/30/2012	4/2/2012*	4/5/2012*	4/9/2012*	4/11/2012*	4/13/2012*	4/16/2012*
Average Reynolds Number	8268	8171	4014	8515	8414	4011	12922	8489	7749	8132	8255	8216	8475
Average Fuel Temperature	-11	-10.8	-10.8	-9.86	-10.2	-10.6	-10.7	-19.3	-7.4	-11.2	-11.1	-7.02	-19.5
Average Rate of Cooling ($\frac{^\circ C}{hour}$)	9.521	10.65	9.3	8.967	9.065	9.991	9.57	8.709	10.59	9.778	8.32	10.13	8.7
Initial Fuel Temperature	21.74	23.15	21.85	22.33	22.3	22.79	21.06	22.97	22	22.23	22.43	20.77	22.16
H_2O Collected from Pipe after Test (mL)	0.103	0.256		1.429	1.248	0.628	0.258	0.086	0.069	0.284			0.127
Test Duration (hrs)	3.204	3.371	3.153	3.273	3.365	3.29	3.26	3.172	3.303	3.269	3.3	3.24	3.17
Total Pressure Rise (Pa)	109.6	191.8	231.3	728.9	700	282.9	763.2	102.3	119.2	314.5	185.2	74.27	107
Normalized Characteristic Pressure Increase	0.17	0.265	0.784	0.709	0.664	1.05	0.335	0.005	0.109	0.274	0.125	0.046	0.029
Rate of Pressure Increase ($\frac{Pa}{m \cdot hr}$)	154.8	213.3	147.8	483.7	407.6	172.9	483.7	132.6	55.08	208.3	82.3	28.96	83.55
Average Flow Rate ($\frac{L}{sec}$)	0.433	0.427	0.21	0.434	0.433	0.208	0.672	0.55	0.372	0.429	0.435	0.391	0.552
Average Viscosity (cSt) ($\cdot 10^6$)	3.189	3.179	3.179	3.102	3.129	3.16	3.167	3.957	2.918	3.211	3.204	2.892	3.968

Table 3.5: Stainless Steel, 3/4″, Top Position (* denotes less contamination)

the CNPI for the 3/4″ insulated tests were within 60% of each other and the CNPI for the 3/4″ un-insulated tests were within 7% of each other.

The volumes of water collected for the 3/4″ insulated tests are within 60% and the volumes of water for the 3/4″ un-insulated pipes were within 13%.

The CNPI values for the remainder of the test cases are shown in tables 3.4 and 3.5.

They show a similar trend.

3.2.3 Temperature Variation

The temperature variation increments were sufficiently spaced to correlate with tests that were done elsewhere by Boeing [3].

Results: Temperature Variation

The three temperature tests were done at approximately the same Reynolds Number. Figures 3.15a, 3.15b and 3.15c are presented to show a qualitative variation of ice accumulation with temperature for the 3/4″ top pipe. Figure 3.15d is given for quantitative representation of the effect of temperature for the 3/4″ top pipe. Qualitative figures are similarly shown for temperature variation of the 1″ top pipe in 3.16.

Discussion: Temperature Variation

Data suggested that there was a relatively small window of temperatures that had the greatest ice accumulation. For the non-insulated case, the normalized pressure for a temperature of -11 °C increased at a rate nearly triple to the temperature of -7.4 °C and about 60 times the temperature of -19.4 °C. These results were consistent with the results of Boeing [3] where they concluded that the ice had a sticky region between -5 °C and -20 °C.

These tests may be used with interpolation to see approximately how ice would accumulate at other temperatures; temperatures less than -19.4 °C would likely have less ice than at -19.4 °C and temperatures greater than -7.4 °C would likely have less accumulation than at -7.4 °C

3.2.4 Reynolds Number Variation

The variation of Reynolds number was spaced to cover the initial portion, the central portion and the final portion of values that might typically be encountered in commercial flights. The smaller Reynolds number value of 3150 is near the transition to turbulence. It would have less turbulent mixing near the pipe wall and less shear stress on the ice. The greater value of 12922 is far into the turbulence regime. It would alternatively have more mixing to the wall and more shear stress on the ice.

Results: Reynolds Number

Comparative images for the variation of Reynolds number with the 3/4″ pipe are shown in figures 3.17a, 3.17b, and 3.17c. Comparative images for variation of Reynolds number for the 1″ pipe are shown in figures 3.18a, 3.18b, and 3.18c. CNPI vs. Re is shown in figure 3.17e for the 3/4″ top pipe. Quantities of water collected are shown in tables 3.4 and 3.5.

Discussion: Reynolds Number

It was apparent from figures 3.17 and 3.18 that as Reynolds number increased, the ice grew progressively thinner. The CNPI correlated with the images and showed that the pressure drop increased more with a thicker ice layer. Figures 3.17d and 3.17e showed that as Reynolds number increased by about 50%, the CNPI decreased by about 40%. Data for the 3/4″ pipe and the 1″ pipe showed the same trend.

3.2.5 Variation of Heat Flux Across the Pipe

This subsection shows quantitative results for the difference in ice accumulation with polyurethane insulation (from chapter 2) on the test pipe and a bare test pipe. To subtract the entrance and exit effects from the pressure data, the normalized pressure

increase of the *insulated* pipe was subtracted from the normalized pressure increase of the *un-insulated* pipe. This would essentially give an effective pipe length equivalent to the length of the insulation. Because the length of the insulation was nearly the same as the pipe, the length parameter in the NCPI was assumed to be the pipe length.

The heat transfer from the pipes was quantified with experimental temperature data and was determined by the temperature difference between the inside and outside walls of the pipes. The fuel temperature was used as the inside pipe temperature and the outside center pipe thermocouple was used for the outside pipe temperature. These temperatures were used with equation 1.5 to calculate the heat transfer.

The inside pipe wall temperature may be more accurately found by the Gnielinski correlation [4]. The correlation is valid for turbulent pipe flow and for a Prandtl number greater than or equal to .5. The relation is shown in equation 3.1. In the equation, Nu_D is the Nusselt number, h_i is the internal convection coefficient, D is the pipe diameter, Re_D is the internal Reynolds number, Pr_f is the Reynolds number of the fuel and f is the internal friction factor. Because the resultant pipe wall temperature would be a small fraction of a degree different than the fuel temperature, they were assumed equal for calculations.

$$Nu_D = \frac{h_i D}{k_f} = \frac{f/8 \cdot (Re_D - 1000) \cdot Pr_f}{1 + 12.7 \cdot (f/8)^{1/2} \cdot (Pr^{2/3} - 1)} \tag{3.1}$$

A theoretical convection heat transfer calculation was also done with approximate air velocity measurements obtained with a hotwire anemometer. The air velocity measurements were used to determine a Reynolds number outside of the pipe. Other appropriate flow parameters such as air viscosity, air Prandtl number, and air thermal conductivity were determined for the specific temperatures. The results of this method are not shown but a qualitative description is given.

Results: Variation of Heat Flux Across the Pipe

Figures 3.19c and 3.19d show the normalized pressure increase in the pipes without insulation and with insulation respectively for the repeatability case. Figure 3.19e shows the difference between them.

The *experimental* heat transfer for the 3/4″ repeatability case is shown for the insulated and un-insulated pipes in figures 3.20a and 3.20b respectively.

The *theoretical* heat transfer from the pipes was calculated and the results showed a similar trend to the experimental results. The magnitude of the theoretical heat transfer was however different than the experimental. The purpose of the heat transfer results was to show how much a percent decrease in heat transfer contributed to a lower ice accumulation. Because the trend in the theoretical case was similar to the trend of the experimental case, the results were not included.

Discussion: Variation of Heat Flux Across the Pipe

As was shown in stage I, the test pipes that were insulated accumulated less ice than the test pipes that were not. The experimental heat transfer results showed that an 85% decrease in heat transfer from the pipe in the 3/4″ pipe repeatability test (T = -11, Re = 8362) led to a 350% decrease in CNPI. The total normalized pressure increase was shown to be 80% larger. The effect of more ice accumulation for test pipes without insulation was true for every test case.

The normalized pressure for the insulated pipe (figure 3.19d) increased initially but leveled off after about an hour. For the first 15 minutes of the tests, the rate of increase of the normalized pressure for the insulated pipe was about the same as the non-insulated pipe. This could be because the ice accumulated more on the pipe unions during this time.

The experimental heat transfer shown in figure 3.20 was determined by the heat transfer in the center of the pipe length (because of the location of the outer pipe

thermocouple) and assumed that the relative temperature differences were uniform along the entire pipe length. If compared to figures 3.19a and 3.19b the relative amount of ice near the center of the pipe length should be used for comparison.

3.2.6 Contamination in the Fuel

At the end of each test when water was melted and collected from the test pipes, there would usually be a small amount of substance that looked like dust and/or metal particles. It was not known initially if this substance facilitated ice accumulation, or if it happened to collect on the pipe also. This substance was observed to dissolve and disappear back into the fuel when the temperature warmed back up to the initial temperature of 21.5 °C. Tests were done to characterize the effect of fuel contamination.

Results: Contamination in the Fuel

Figures 3.21a and 3.21b show the qualitative effect of more vs. less contamination in the fuel. Figures 3.21c and 3.21d show comparative results for the normalized pressure increase for the two cases. The amount of water collected for the two contamination cases is shown in tables 3.4 and 3.5. An image of some of the contaminant is shown in figure 3.22.

Discussion: Contamination in the Fuel

A greater level of contamination in the fuel increased the amount of ice that accumulated. The CNPI for the less contaminated pipe was .139. The CNPI for the more contaminated pipe was .3155. The case that had less contamination still had some contamination and was observed when the ice was melted. Some of the entrained water in the fuel was speculated to have used the contaminant as a nucleus and contributed to soft ice.

This contamination may have come in three forms in addition to what was present in the fuel upon delivery. For some of the time that the gear pump was used, the gears may not have been aligned properly and metal deposits could have resulted. Some of the fuel that leaked out of the system and was later pumped back in (described in section 2) could have acquired dust in the process. Finally, when the pipe system was assembled, aluminum particles from the pipes could have entered the flow.

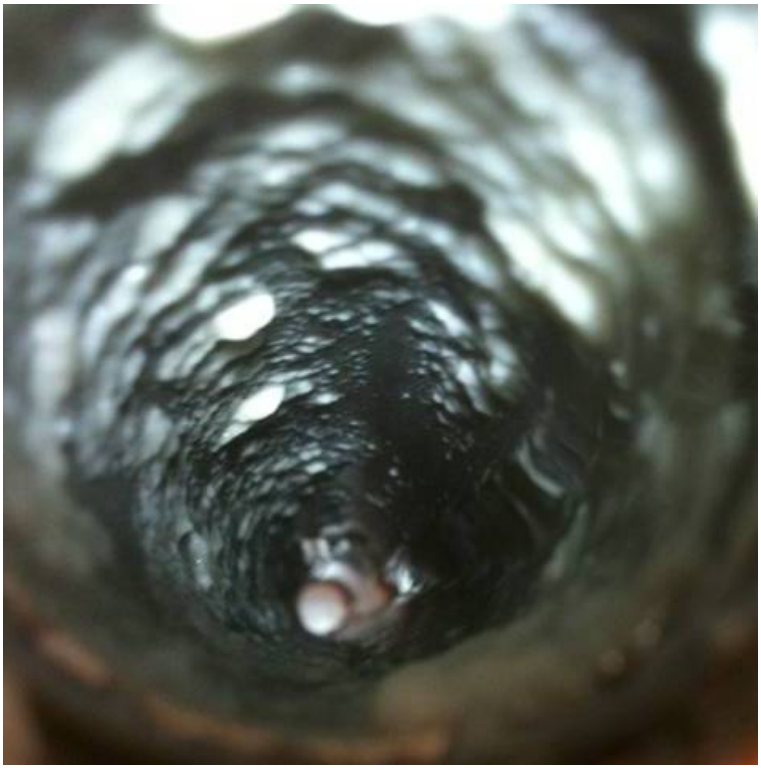

(a) Results from Initial Condition 1

(b) Results from Initial Condition 2

Figure 3.1: Variation of Initial Conditions

(c) Results from Initial Condition 3

(d) Results from Initial Condition 4 (Before the test)

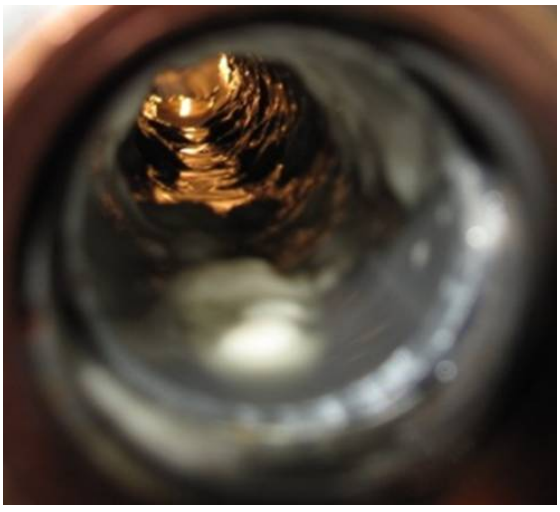

(e) Results from Initial Condition 4 (After the test)

Figure 3.1: Variation of Initial Conditions

(a) Saturated Fuel

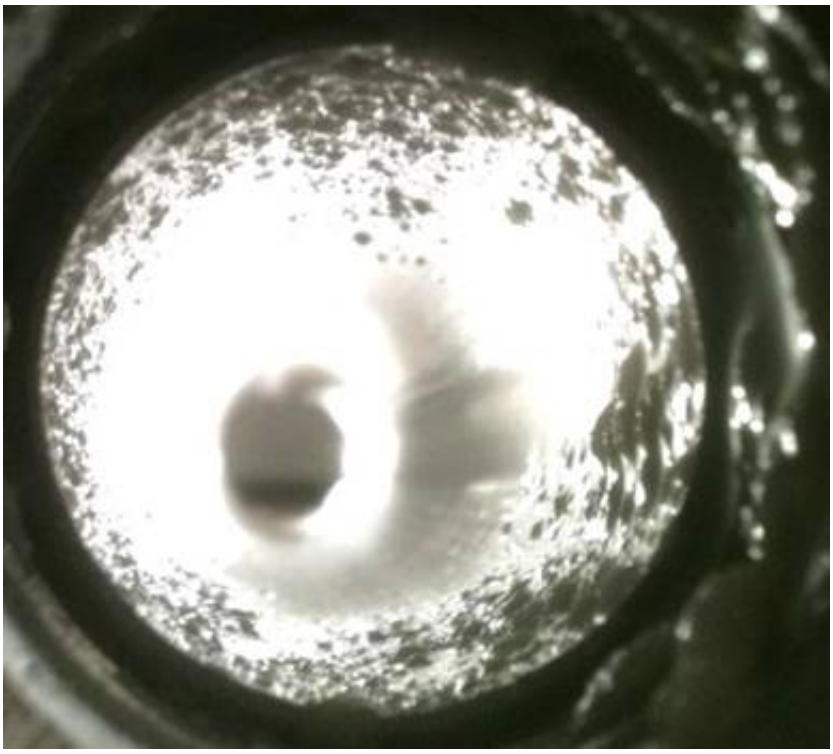

(b) Saturated Fuel with Extra Emulsified Water

Figure 3.2: Saturated Fuel and Supersaturated Fuel Comparison, Re = 2000, T = -8.7 °C

(a) Teflon® (top pipe)

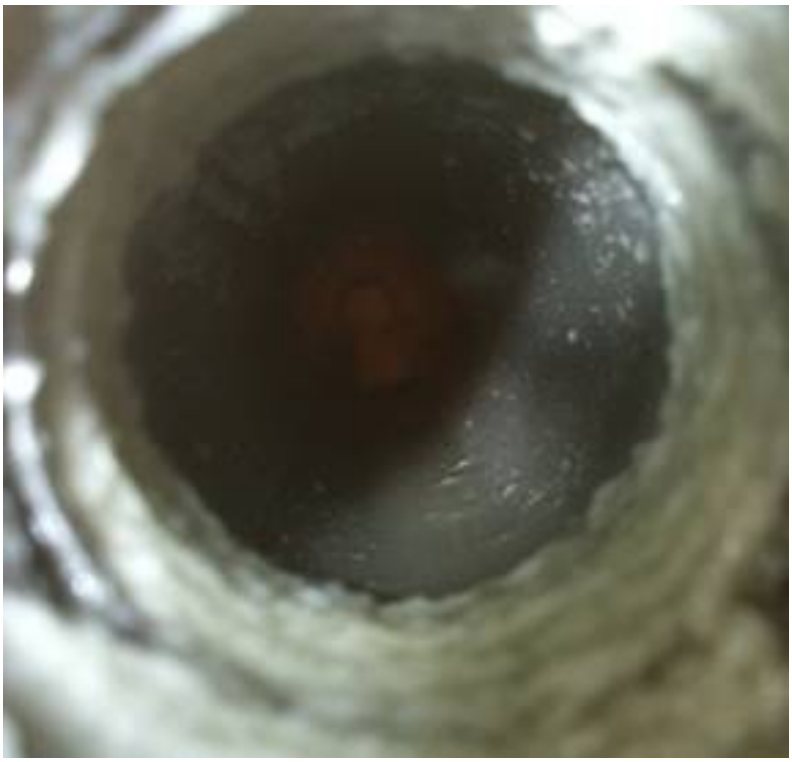

(b) Stainless Steel (bottom pipe)

Figure 3.3: Teflon® and Stainless Steel Comparison, Re = 2024, T = -9.5 °C

(a) Stainless Steel (Bottom Pipe)

(b) Scratched Aluminum (Top Pipe)

Figure 3.4: Stainless Steel and Scratched Aluminum Comparison, Re = 5975, T = -9.5 °C

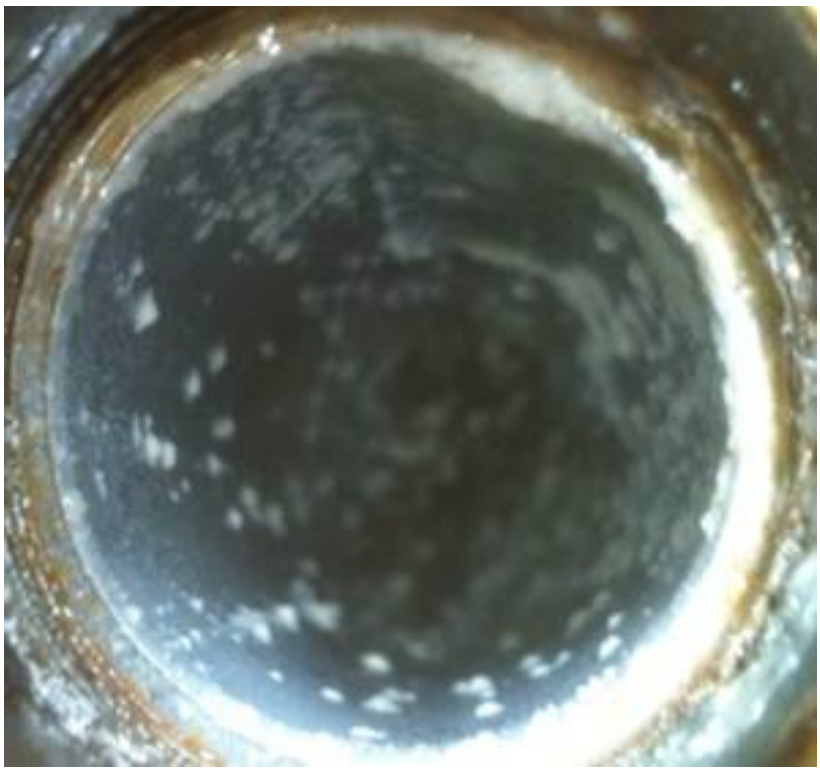

(a) Downstream of 2 $\frac{1}{4}''$ radius pipe bend

(b) Downstream of 1 $\frac{1}{4}''$ radius pipe bend

Figure 3.5: 2 $\frac{1}{4}''$ and 1 $\frac{1}{4}''$ radius pipe bends

(a) Un-Insulated, Downstream

(b) Insulated, Upstream

Figure 3.6: Insulated vs. Un-Insulated Scratched Aluminum

(a) Un-Insulated, Downstream

(b) Insulated Upstream

Figure 3.7: Insulated vs. Un-Insulated Teflon®

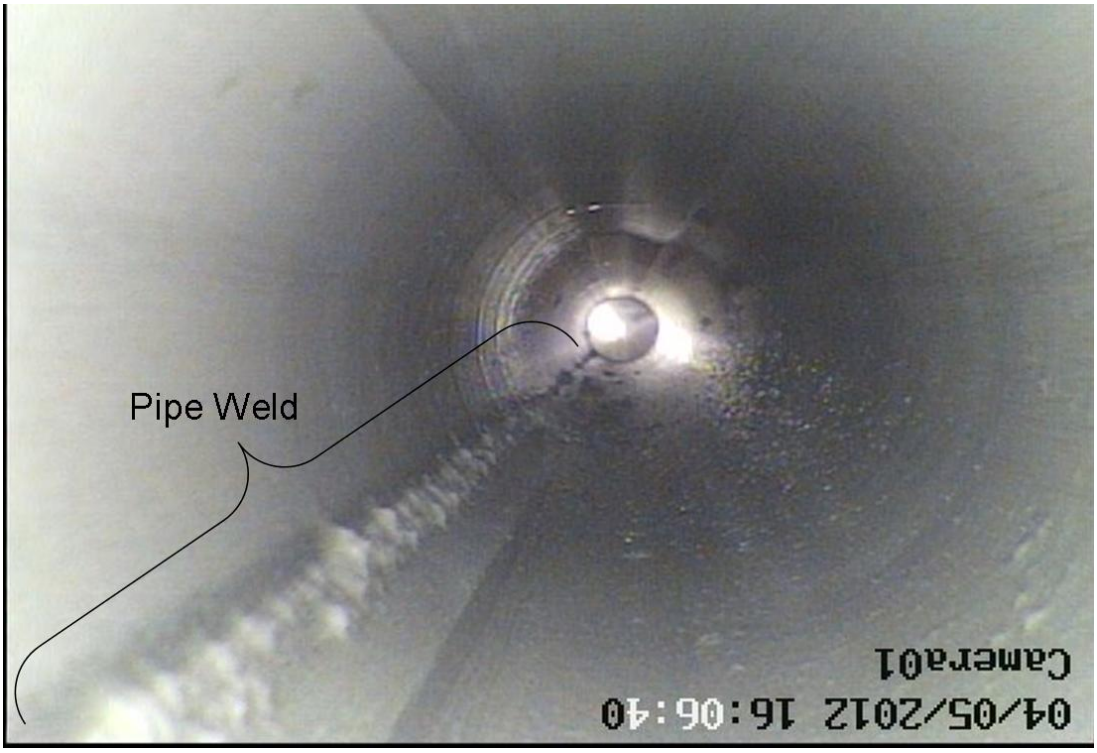

(a) Pipe Oriented up-side-down, T = -7.4 °C, Downstream

(b) Pipe Oriented right-side-up, T = -11 °C, Downstream

Figure 3.8: Illustration that Ice had a Tendency to Accumulate on Welds Independent of Orientation, Re = 6568, Bottom Position

(a) Upstream Pipe Section

(b) Downstream Pipe Section

Figure 3.9: Difference between Upstream and Downstream Re = 6568, T = -11 °C, 1″, Un-Insulated Stainless Steel, Bottom Position

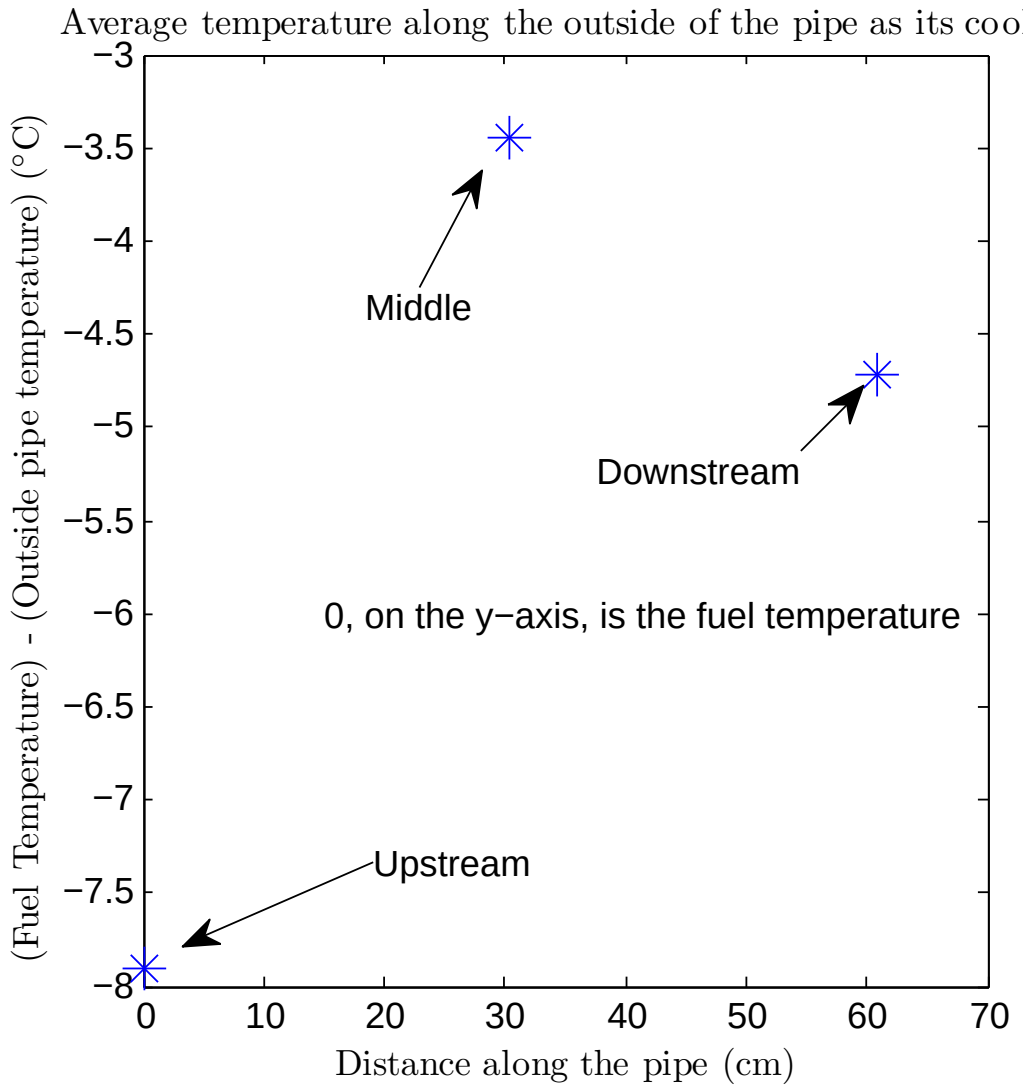

Figure 3.10: Approximate temperature on the outside of the bottom pipe

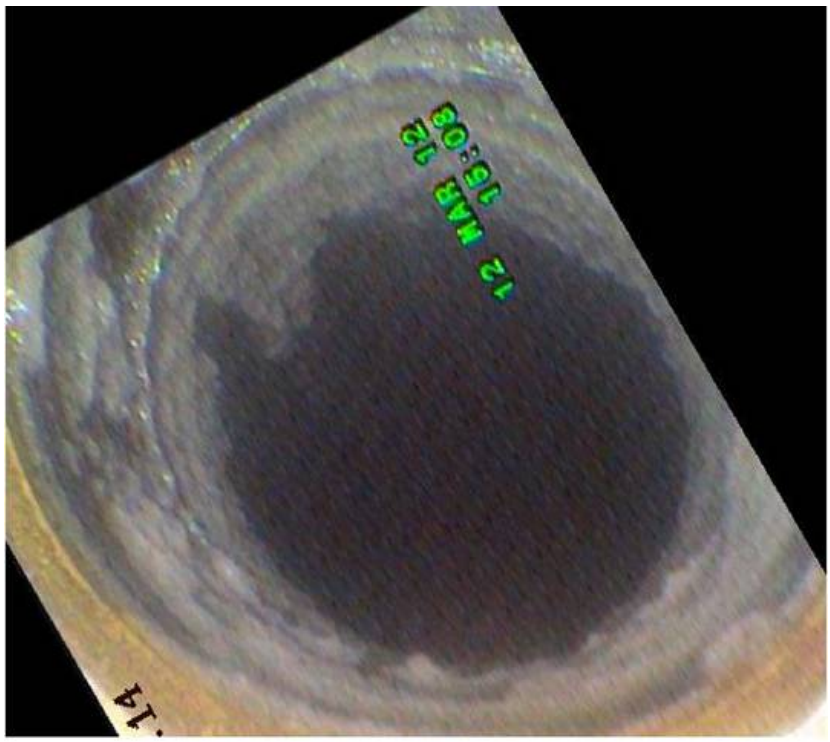

(a) Test 1, Upstream

(b) Test 2, Upstream

Figure 3.11: Repeatability, Re = 6568, T = -11 °C, 1″ Insulated Stainless Steel, Bottom Position

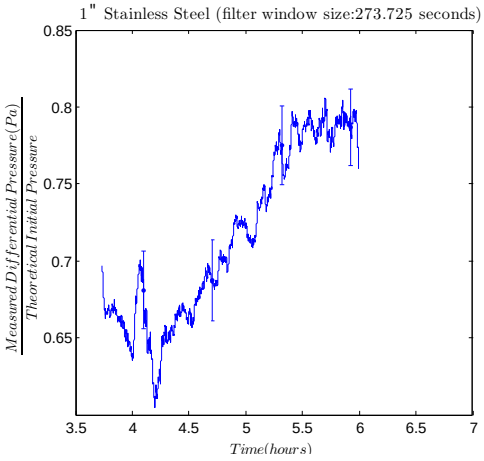

(c) Test 1 (03-12-12)

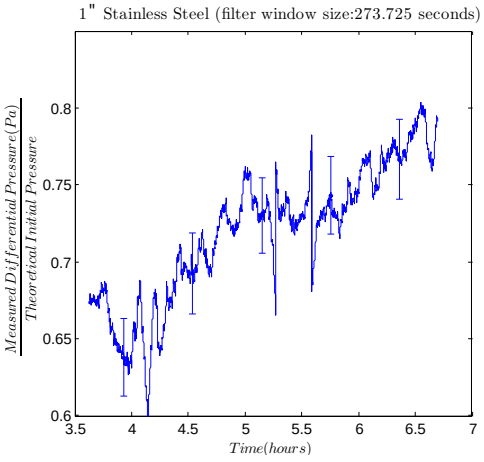

(d) Test 2 (03-15-12)

Figure 3.11: Repeatability, Re = 6568, T = -11 °C, 1″ Insulated Stainless Steel, Bottom Position

(a) Test 1, Upstream

(b) Test 2, Upstream

Figure 3.12: Repeatability, Re = 6568, T = -11 °C, 1″ Un-Insulated Stainless Steel, Bottom Position

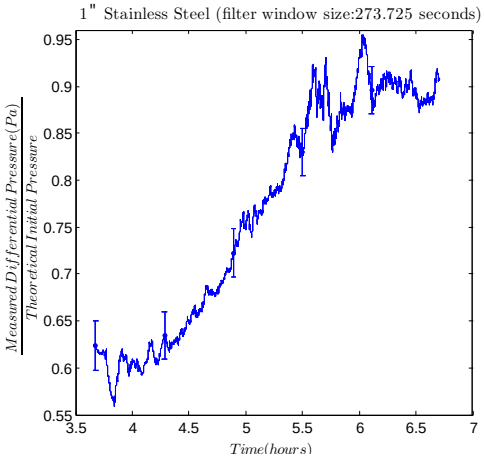

(c) Test 1 (03-22-12)

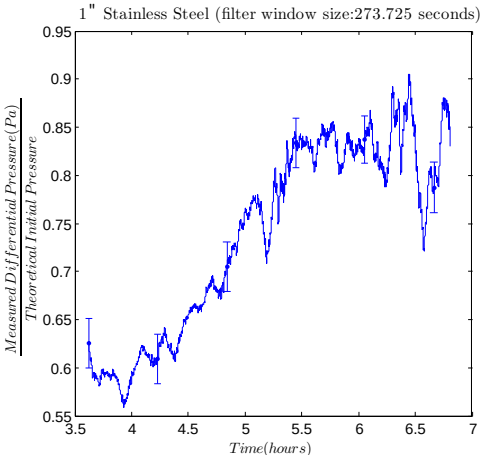

(d) Test 2 (03-26-12)

Figure 3.12: Repeatability, Re = 6568, T = -11 °C, 1″ Un-Insulated Stainless Steel, Bottom Position

(a) Test 1, Downstream

(b) Test 2, Downstream

Figure 3.13: Repeatability, Re = 8362, T = -11 °C, 3/4″ Un-Insulated Stainless Steel, Top Position

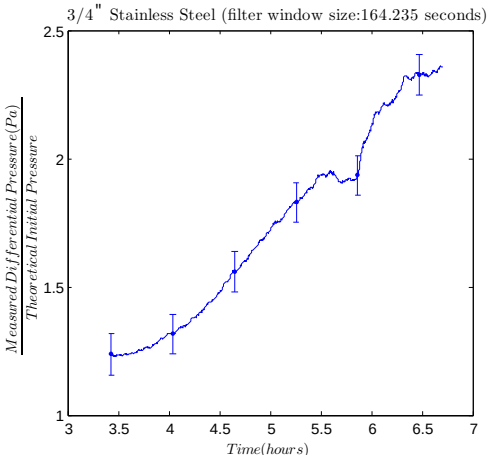

(c) Test 1 (03-22-12)

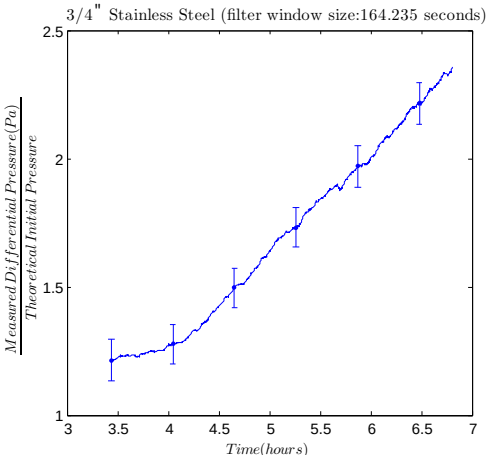

(d) Test 2 (03-26-12)

Figure 3.13: Repeatability, Re = 8362, T = -11 °C, 3/4″ Un-Insulated Stainless Steel, Top Position

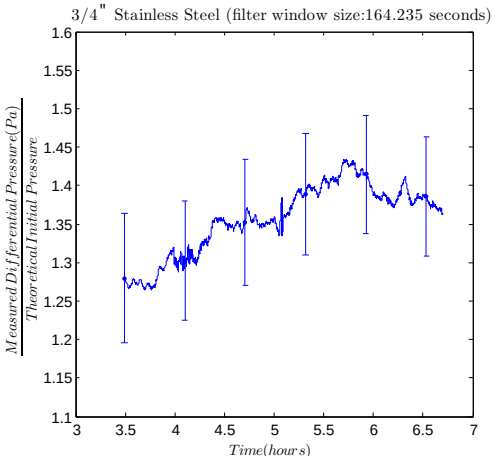

(a) Test 1 (03-12-12)

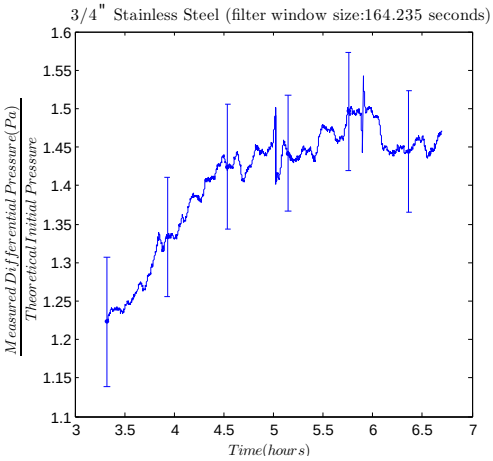

(b) Test 2 (03-15-12)

Figure 3.14: Repeatability, Re = 8362, T = -11 °C, 3/4″ Insulated Stainless Steel, Top Position

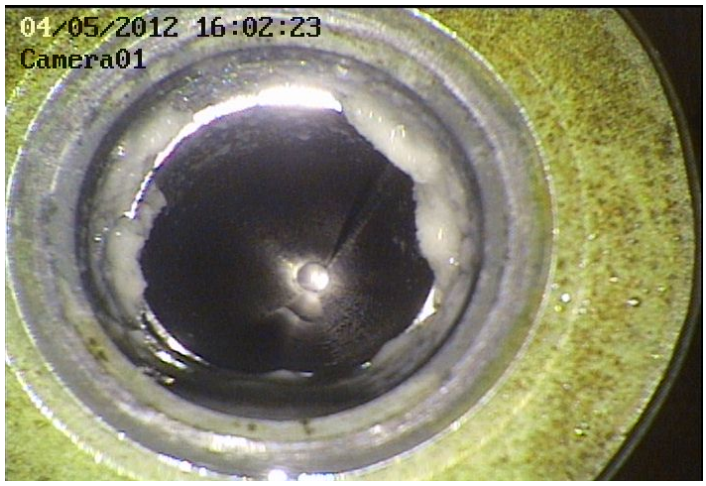

(a) T = -7.4 $^{\circ}C$ upstream

(b) T = -11.24 $^{\circ}C$ upstream

(c) T = -19.4 $^{\circ}C$ upstream

Figure 3.15: Temperature Variation, Re = 8362, 3/4″ Un-Insulated Stainless Steel, Bottom Position

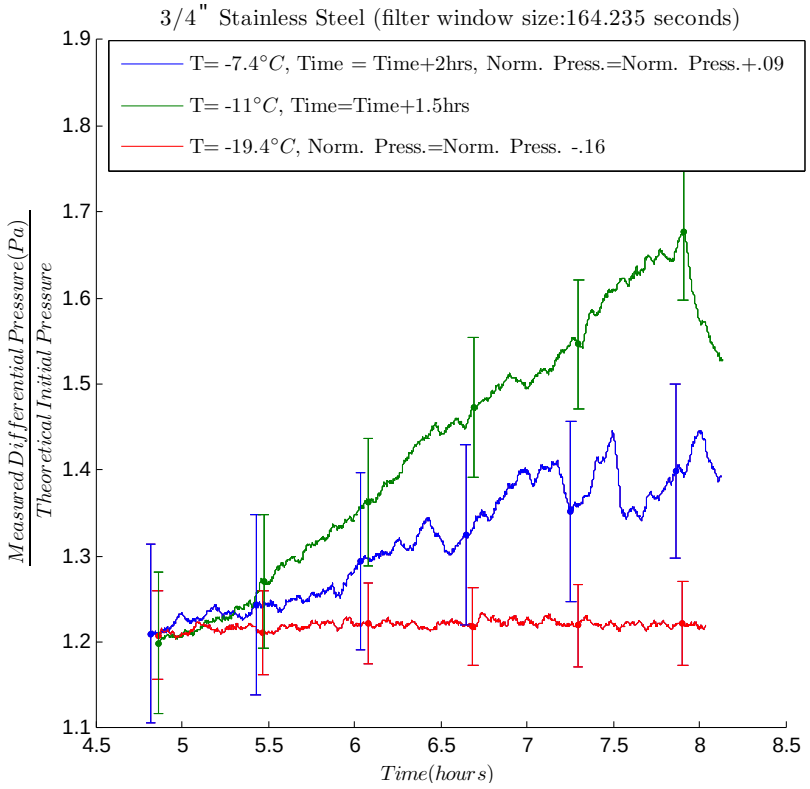

(d)

Figure 3.15: Temperature Variation, Re = 8362, 3/4″ Un-Insulated Stainless Steel, Bottom Position

(a) T = -7.4 $^{\circ}C$, Upstream

(b) T = -11.24 $^{\circ}C$, Upstream

(c) T = -19.35 $^{\circ}C$, Upstream

Figure 3.16: Temperature Variation, Re = 6568, 1″ Un-Insulated Stainless Steel, Bottom Position

(a) Re= 4000, Upstream

(b) Re= 8362, Upstream

(c) Re= 12922, Upstream

Figure 3.17: Reynolds Number Variation, T = -11 °C, 3/4″ Un-Insulated Stainless Steel, Top Position

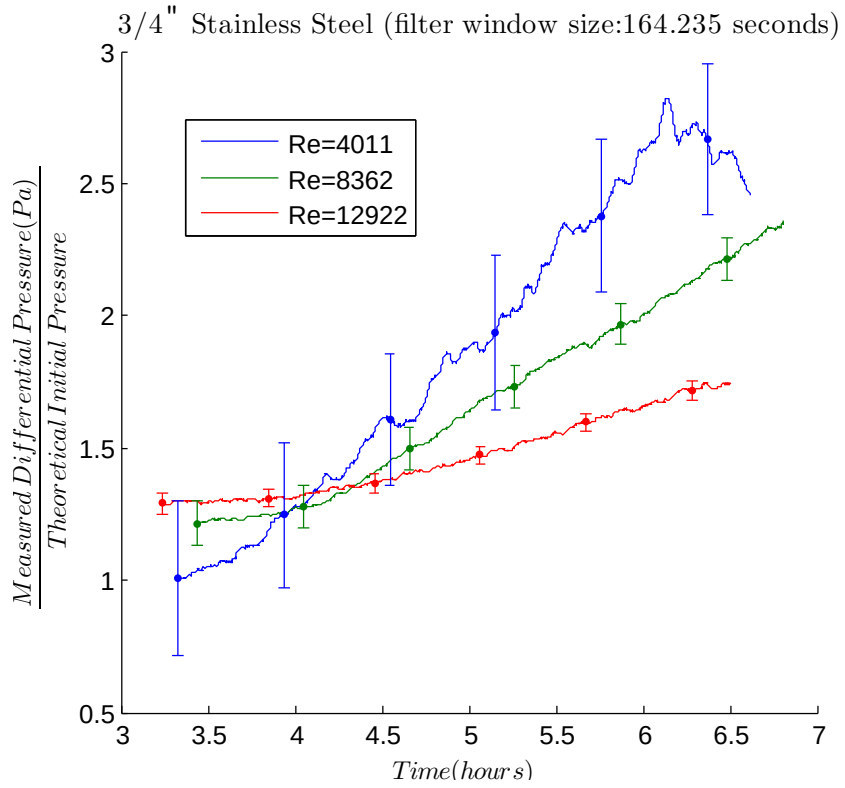

(d)

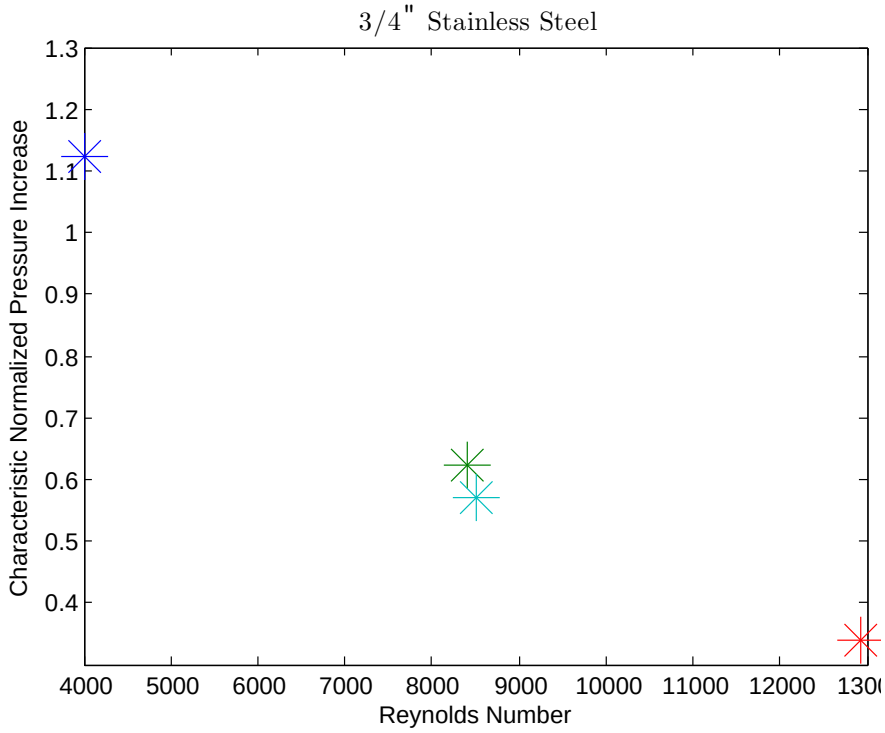

(e)

Figure 3.17: Reynolds Number Variation, T = -11 °C, 3/4″ Un-Insulated Stainless Steel, Top Position

(a) Re= 3150, Upstream

(b) Re= 6568, Upstream

(c) Re= 10150, Upstream

Figure 3.18: Reynolds Number Variation, T = -11 °C, 1″ Un-Insulated Stainless Steel, Bottom Position

(a) 3/4″ Un-Insulated Stainless Steel, Downstream

(b) 3/4″ Insulated Stainless Steel, Downstream

Figure 3.19: Insulated vs. Un-Insulated, Re = 8362, T = -11 °C, 3/4″ Stainless Steel, Bottom Position

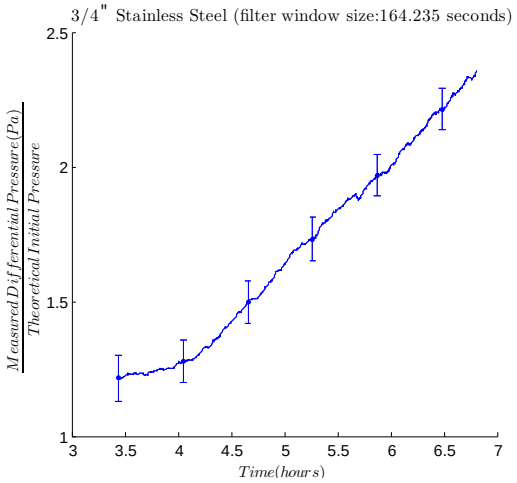

(c) Un-Insulated

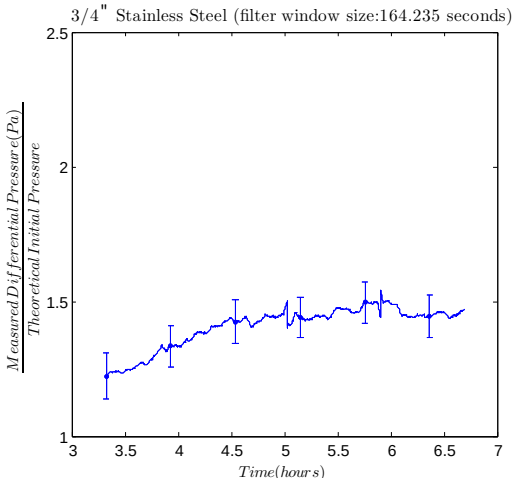

(d) Insulated

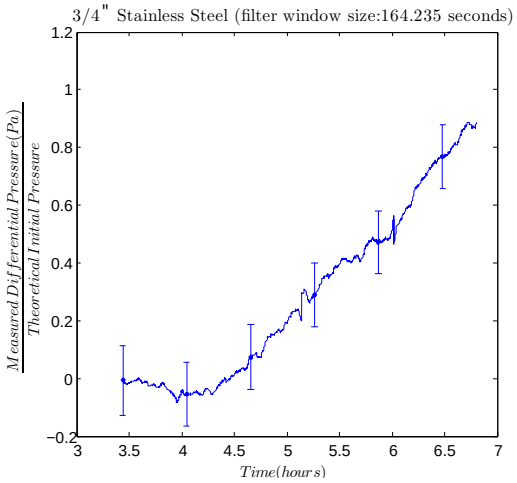

(e) (Un-Insulated) - (Insulated)

Figure 3.19: Insulated vs. Un-Insulated, Re = 8362, T = -11 °C, 3/4″ Stainless Steel, Bottom Position

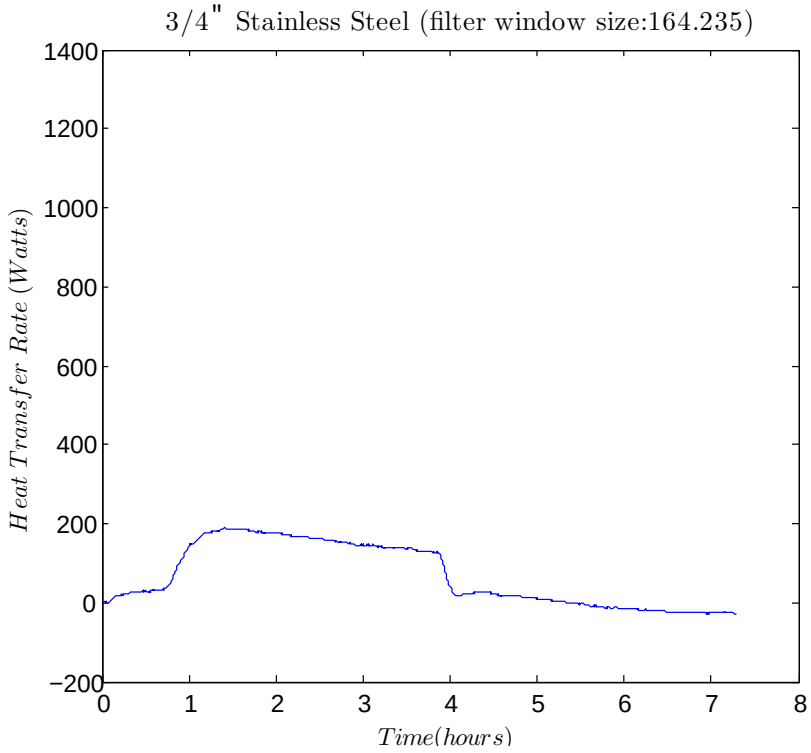

(a) Insulated

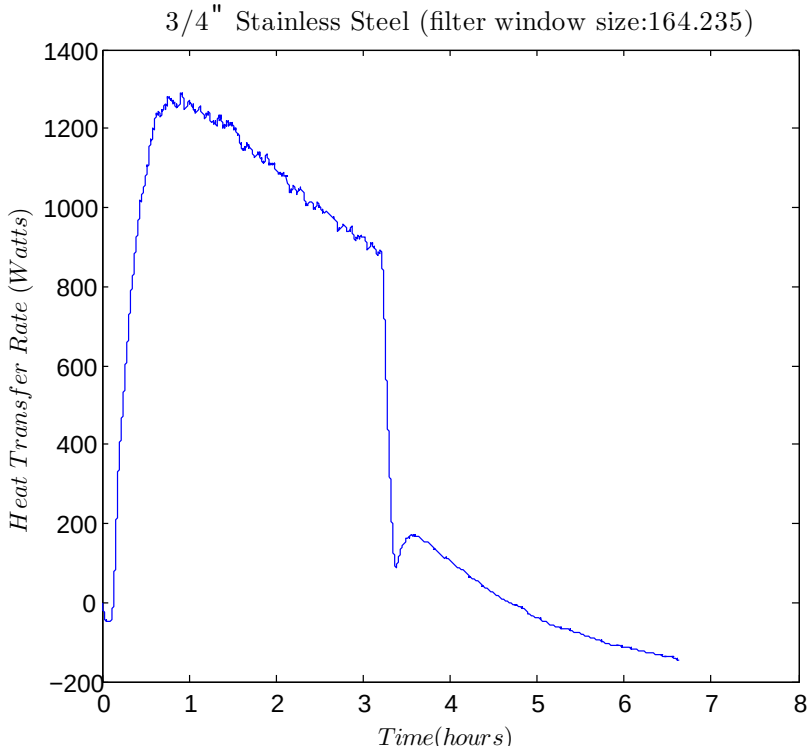

(b) Un-insulated

Figure 3.20: Insulated and Un-Insulated Experimental Heat Transfer Rates, Re = 8362, T = -11 °C, 3/4″

(a) More Contaminated, Upstream

(b) Less Contaminated, Upstream

Figure 3.21: More Contaminated vs. Less Contaminated Fuel, Re = 6568, T = -11 °C, 1″ Un-Insulated Stainless Steel, Bottom Position

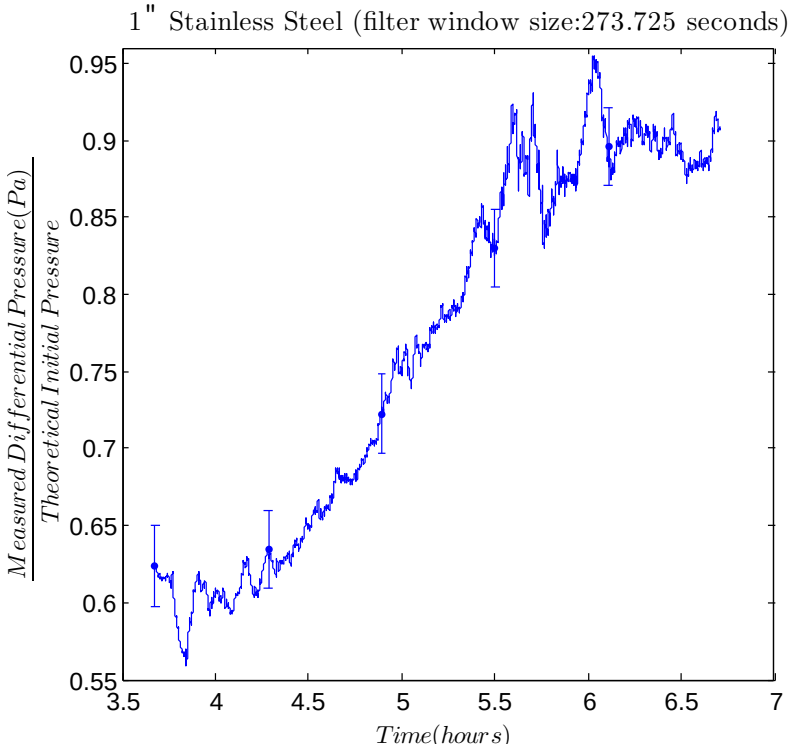

(c) More Contaminated

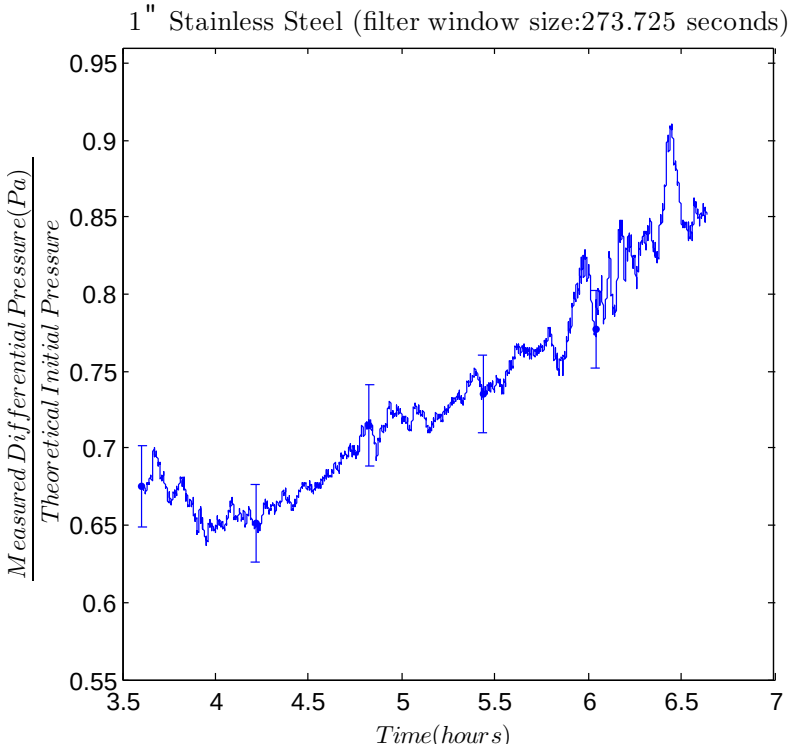

(d) Less Contaminated

Figure 3.21: More Contaminated vs. Less Contaminated Fuel, Re = 6568, T = -11 °C, 1″ Un-Insulated Stainless Steel, Bottom Position

Figure 3.22: Contamination

4. Error Analysis

4.1 Uncertainty

In stage II uncertainty analysis was done in MATLAB for each test for each of the calculated parameters. The equipment uncertainty was used with equation 4.1. The resultant error bars were shown in the pressure plots. In the calculations, flow rate uncertainty ignored errors from the bucket test calibration.

$$u = \sqrt{u_{a1}\frac{du}{da_1} + u_{a2}\frac{du}{da_2} + u_{a3}\frac{du}{da_3} + ...} \tag{4.1}$$

4.2 CNPI and Pressure Rise

The CNPI was determined by selection of two points on a normalized pressure plot. The selected points were based upon judgment and the resultant CNPI could vary about 10% as a result.

The total pressure rise, from tables 3.4 and 3.5 was also determined by the selection of points on a plot. The total pressure rise may have repeatability error of about 5%.

4.3 Heat Transfer Through the Pipe

The experimental heat transfer results depended on a temperature difference of a few degrees Celsius from the type T thermocouples. This temperature difference was

approximately the same as the accuracy of the thermocouples. This was a source of error.

The center outside pipe thermocouple may not have determined a true outside pipe temperature. The thermocouple had a relatively small amount of surface contact to the test pipe compared to the surface contact it had with the ambient air. The change due to this effect would however seem minimal because conduction through stainless steel has greater heat transfer than convection of air in the conditions of these tests.

The inner pipe temperature in the experimental heat transfer analysis assumed that the fuel temperature immediately downstream of the test pipe was representative of the fuel temperature in the entire test pipe. Because the heat transfer was unsteady and the fuel temperature dropped as it traveled through the pipe, this was not exact. However, because the Reynolds number inside the pipe was as high as it was, the fuel temperature change along the pipe was assumed negligible. The experimental heat transfer error may be near 100% or greater.

The error for the theoretical heat transfer results were dependent on the hotwire accuracy, the fuel and chamber thermocouple accuracies, and the accuracy of the model. These errors may be compared with the experimental heat transfer error to account for the difference in heat transfer magnitude from the theoretical and experimental models.

4.4 Other Sources of Error

Because two of the outside thermocouples for the bottom pipe were "home made" their accuracy may be different than the other thermocouples.

There may have been error with the water content of the fuel. It is possible that the initial water content of the fuel varied within a few ppm.

For many of the tests the pump displayed oscillatory behavior. The data filter that was incorporated, smoothed most of this behavior. The motor and pump were

mounted inside the chamber on an aluminum plate. When the chamber cooled the plate would change size and slightly affect the alignment of the motor. The pump oscillations usually remained consistent and would tend to only affect the uncertainly of the system flow rate. The pulsed increase and decrease in shear stress from the oscillations may be considered small compared to the mean shear stress.

In figures 3.11d and 3.14b, the data had excess noise. The noise was subtracted from the figures.

Finally, another source of error that may have existed was with the water measurements at the end of each test. It is possible that some of the condensation from air that accumulated on the outside of the pipe when it was taken out of the chamber dripped into the water collection tray (figure 2.8). Care was however taken to prevent this. If a drop did fall into the tray it could have contributed about .05 mL to the results. It was certain that this did not happen to about 95% of the tests.

5. Conclusions

5.1 Summary of Results

There were discoveries that resulted from this study:

- The initial condition tests showed that the soft ice collected on hard ice. As the system cooled the hard ice was created from entrained water in the fuel.
- A greater amount of emulsified water in the fuel corresponded to greater ice accumulation.
- Stainless steel accumulated more ice than Teflon® and apparently more than scratched aluminum.
- An increase in heat transfer from the fuel pipe increased ice accumulation.
- Pipe bends were not shown to create a preferential ice accumulation region.
- Contamination in the fuel from particles was shown to increase ice accumulation.
- Ice had a greater tenancy to accumulate at -11 °C than at -7.4 °C or -19.4 °C
- Finally, lower flow rates contributed to thicker ice layers.

In this study, the convection coefficient was greater for the top pipe than the bottom pipe. At ambient conditions colder than the fuel, a greater convection coefficient

led to a greater heat loss from the pipe and was shown in this study to increase ice accumulation.

The average amount of total water collected from both test pipes after each test was .608mL. If the initial water content was 100ppm at 21.5 $^{\circ}C$, the average combined H_2O accumulation from both of the test pipes was 1.4% of the initial quantity present in the fuel. A decrease in ice accumulation rate because of a decrease in the water content of the system was considered negligible.

5.2 Application to Industry

Ice may break off of surfaces instantaneously from many individual areas or from a single large collection. Some of the dips in the pressure data suggested that the ice broke from the pipe while the tests were in progress. For aircraft safety, small ice releases would be of lesser concern.

A possible solution to reduce ice collection in fuel pipes is to insulate them. Other solutions may include a change in the pipe material or a decrease in the distance that the fuel has to travel before it reaches the FOHE or other areas that may clog.

Several circumstances may be considered to be of greater risk for high ice accumulation. The softer type of ice is the main fuel component clogger. The soft ice is likely frozen entrained water. If fuel below 0 °C is loaded onto an airplane it is likely to contain a high amount of soft ice.

If, on the previous flight, prior to the refuel, the fuel temperature on the aircraft had decreased from above 0 °C to below 0 °C then the pipes are likely to have a layer of harder ice. The large quantity of soft ice in the new fuel is likely to stick to the layer of hard ice.

If the fuel is cold enough, a large quantity of ice may not have to break free from the system at once to clog a FOHE. Ice could break free in relatively small quantities and slowly collect on the face of the heat exchanger.

5.3 Future Work

There is much work that can be done to increase what is known about ice accumulation in fuel pipes. Further changes may be made to the fuel and to the test pipe. Experiments for the determination of ice release mechanisms may be explored. Scenarios such as the sudden release of a large quantity of ice or water may be tested and additional tests may be done to further characterize the type of ice that accumulates.

Additives

Changes that may be made to the fuel include the addition of components such as those mentioned in 1.2.3. They include: static dissipater additive, antioxidant, metal deactivator, lubricity additive, fuel system icing inhibitor, +100 additive, organic compounds containing sulfur, nitrogen, or oxygen, trace amounts of metals and microbial growth. It should be noted that fuel system icing inhibitor (FSII) was previously tested at the FAA technical center, but for future work the concentration of FSII may be varied.

Other Fuels

More than the addition of additives, other fuels may be tested such as Jet-A or other samples of Jet A-1. These fuels may further be examined to see what their hydrocarbon constituents are and an analysis may be done to see how they individually contribute to ice accumulation. This would add to previous work that was done for water retention of these components by [14].

Initial Water Content

Additional data could be compiled to quantitatively determine the effect of additional water emulsion in fuel.

Slug of Water

The sudden release of a water slug into a fuel system at cold temperature may be of interest. Experiments could be done to determine its effect on downstream flow components such as filters or fuel oil heat exchangers (FOHE's).

Heat Transfer Variation

The heat transfer from the pipe could be varied and quantified for a determination of its dependence on ice accumulation. Different insulations with various thermal resistances could be used to determine upper and lower bounds of thermal resistances that would be optimally effective.

Future Work with this Setup

There are things that could be changed with the experimental setup used for this study. The oscillations of the pump may not have contributed significantly to the overall ice accumulation, but in the future, the pump and motor could be taken out of the chamber so that their alignment would stay constant and the thermal expansion of the mount would not be a variable.

Stickiness of the Ice

Tests could be done to further investigate the stickiness of the soft ice. It may be of interest to see if ice would release from a pipe surface if the fuel temperature was lowered. This could be done quantitatively with differential pressure measurements.

Accumulation on Welds

More could be done to quantify the tendency for ice to accumulate on welds. Another series of tests could be done with extruded schedule 80 stainless steel pipe to compare ice accumulation rates.

Full Scale Flight Tests

Flight tests could be done in full scale. An aircraft may be fitted with a differential pressure transducer in its pipe system and flight tests may be done with and without insulation and with other pipe materials or conditions.

Electric Fields

An electric field may be applied to the test pipe and the rate of ice accumulation may be quantified.

References

[1] C. Allain, D. Ausserre, and F. Rondelez. "A new method for contact-angle measurements of sessile drops". In: *Journal of colloid and interface science* 107.1 (1985), pp. 5–13.

[2] Exxon Mobil Aviation. *World Jet Fuel Specifications with Avgas Supplement*. 2008. URL: `http://www.exxonmobilaviation.com/AviationGlobal/Files/WorldJetFuelSpec2008_1.pdf`.

[3] Boeing. *Air Accident Report: 1/2010 G-YMMM*. Tech. rep. 2010.

[4] GP Celata et al. "Single-phase laminar and turbulent heat transfer in smooth and rough microtubes". In: *Microfluidics and Nanofluidics* 3.6 (2007), pp. 697–707.

[5] Martin Chaplin. *Ice phases*. 2012. URL: `http://www.lsbu.ac.uk/water/ice.html`.

[6] Coordinating Research Council. "Handbook of Aviation Fuel Properties (CRC Report No. 635)". In: (2004).

[7] E Corporan and M DeWitt. "Chemical, thermal stability, seal swell and emission characteristics of jet fuels from alternative sources." In: *11th International Conference on Stability, Handling and Use of Liquid Fuels*. 2009.

[8] EASA. *Proposed Deviation on Water icing in fuel Applicable to Airbus A330 / A340*.

[9] R. Gouni. "A New Technique to Study Temperature Effects on Ice Adhesion Strength for Wind Turbine Materials". PhD thesis. Case Western Reserve University, 2011.

[10] P.V. Hobbs. "Ice physics". In: *Oxford: Clarendon Press, 1974* 1 (1974).

[11] American Petroleum Institute. *Robust summary of information on Kerosene/Jet Fuel*. 2003. URL: http://www.epa.gov/hpv/pubs/summaries/kerjetfc/c15020rs.pdf.

[12] HH Jellinek. *Adhesive Properties of Ice. Part 2*. Tech. rep. DTIC Document, 1960.

[13] R.E. Kirk and D.F. Othmer. *Encyclopedia of chemical technology: Antibiotics (Phenazines) to Bleaching agents*. Encyclopedia of Chemical Technology. Wiley, 1978. ISBN: 9780471020394. URL: http://books.google.com/books?id=89A2AAAAMAAJ.

[14] J.A. Krynitsky, J.W. Crellin, and H.W. Carhart. *The Behavior of Water in Jet Fuels and the Clogging of Micronic Filters at Low Temperatures*. Tech. rep. DTIC Document, 1950.

[15] C. Laforte and A. Beisswenger. "Icephobic material centrifuge adhesion test". In: *11 th International Workshop of Atmospheric Icing on Structure, Montréal*. 2005.

[16] L. Lao et al. "Behaviour of Water in Jet Fuel in a Simulated Fuel Tank". In: *SAE Technical Paper* (2011), pp. 01–2794.

[17] K. Manohar and K. Ramroop. "A Comparison of Correlations for Heat Transfer from Inclined Pipes". In: *International Journal of Engineering (IJE)* 4.4 (2010), p. 268.

[18] MATLAB. *Matlab Help Files, student version 7.12.0 (R2011a)*. Natick, Massachusetts: The MathWorks Inc., 2011.

[19] Benjamin J. Murray, Sarah L. Broadley, and G. John Morris. "Supercooling of Water Droplets in Jet Aviation Fuel". In: *Fuel* 90.1 (2011), pp. 433 –435. ISSN: 0016-2361. DOI: 10.1016/j.fuel.2010.08.018. URL: http://www.sciencedirect.com/science/article/pii/S0016236110004345.

[20] K. Nitsch. "Thermal analysis study on water freezing and supercooling". In: *Journal of Thermal Analysis and Calorimetry* 95.1 (2009), pp. 11–14.

[21] V. Petkov, Y. Ren, and M. Suchomel. "Molecular arrangement in water: random but not quite". In: *Journal of Physics: Condensed Matter* 24 (2012), p. 155102.

[22] pro-act. *Petroleum Fuels: Basic Composition and Properties*. 1999. URL: http://infohouse.p2ric.org/ref/07/06026.htm.

[23] Leonard R. Scotty. "Above and Beyond: Fire and Ice". In: *Air and Space magazine* (2010).

[24] D. Standard. "91-91". In: *Turbine Fuel, Aviation Kerosene Type, Jet A-1 NATO Code: F-35 Joint Service Designation: AVTUR* (18 2011).

[25] G. Vali. "Ice Nucleation-Theory: A Tutorial". In: *NCAR/ASP 1999 Summer Colloquium*. 1999.

[26] Wikipedia. *British Airways Flight 38 — Wikipedia, The Free Encyclopedia*. [Online; accessed 16-April-2012]. 2012. URL: http://en.wikipedia.org/w/index.php?title=British_Airways_Flight_38&oldid=486312281.

[27] Wikipedia. *Contact angle — Wikipedia, The Free Encyclopedia*. [Online; accessed 16-April-2012]. 2012. URL: http://en.wikipedia.org/w/index.php?title=Contact_angle&oldid=477926512.

[28] Wikipedia. *Ice — Wikipedia, The Free Encyclopedia*. [Online; accessed 16-April-2012]. 2012. URL: http://en.wikipedia.org/w/index.php?title=Ice&oldid=487515525.

[29] Wikipedia. *Troposphere — Wikipedia, The Free Encyclopedia*. [Online; accessed 29-April-2012]. 2012. URL: http://en.wikipedia.org/w/index.php?title=Troposphere&oldid=488927311.

[30] Wikipedia. *Wetting — Wikipedia, The Free Encyclopedia*. [Online; accessed 11-May-2012]. 2012. URL: http://en.wikipedia.org/w/index.php?title=Wetting&oldid=491719768.

[31] AH Yavrouian, M. Sarbolouki, and V. Sarohia. *Influence of Liquid Water and Water Vapor on Antimisting Kerosene (AMK)*. Tech. rep. DTIC Document, 1983.